



DEVELOPMENT OF MICROFLUIDIC TOOLS FOR STUDYING INDIVIDUAL  
ZOOPLANKTONS



A Thesis Submitted to the Graduate School of Naresuan University  
in Partial Fulfillment of the Requirements  
for the Master of Science in Biochemistry

2022

Copyright by Naresuan University

DEVELOPMENT OF MICROFLUIDIC TOOLS FOR STUDYING INDIVIDUAL  
ZOOPLANKTONS



A Thesis Submitted to the Graduate School of Naresuan University  
in Partial Fulfillment of the Requirements  
for the Master of Science in Biochemistry  
2022  
Copyright by Naresuan University

Thesis entitled "Development of microfluidic tools for studying individual zooplanktons"

By Dusitta Detkeow

has been approved by the Graduate School as partial fulfillment of the requirements for the Master of Science in Biochemistry of Naresuan University

**Oral Defense Committee**

..... Chair  
( Nukul Saengphan, Ph.D.)

..... Advisor  
( Pakpoom Subsoontorn, Ph.D.)

..... Internal Examiner  
(Assistant Professor Amnat Phetrungnapha, Ph.D.)

..... Internal Examiner  
(Assistant Professor Chayaphon Sriphannam, Ph.D.)

**Approved**

.....  
(Associate Professor Krongkarn Chootip, Ph.D.)  
Dean of the Graduate School

<b>Title</b>	DEVELOPMENT OF MICROFLUIDIC TOOLS FOR STUDYING INDIVIDUAL ZOOPLANKTONS
<b>Author</b>	Dusitta Detkeow
<b>Advisor</b>	Pakpoom Subsoontorn, Ph.D.
<b>Academic Paper</b>	M.S. Thesis in Biochemistry, Naresuan University, 2022
<b>Keywords</b>	Microfluidic, Zooplanktons, Image Analysis

### ABSTRACT

Zooplanktons are the foundation of aquatic food chains and extensively used as aquaculture live feeds. Exploration and utilization of zooplankton diversity would expand our understanding of aquatic ecosystems and benefit the aquaculture industry. Nonetheless, current methods for isolating and studying diversity of individual zooplanktons remain slow and labor intensive. The objective of this study was to develop a microfluidic device and image analysis software for studying and isolating individual zooplanktons. We built a microfluidic chip from acrylic/PDMS sheets and used a water dipping system to control zooplankton flow. Image analysis software, based on Python OpenCV, automatically measured size and color of individual zooplanktons. A solenoid valve, coupled to a microcontroller, allowed experimenters to manually isolate selected zooplanktons. Our device flows a single stream of tested zooplankton, *Moina macrocopa*, across our chip and allowed isolation of individual zooplankton. Size and grayscale color of individual zooplankton measured by our automated software are well-correlated with manual measurement. Our device can isolate *M. macrocopa* by size and color with 75-85% and 80-85% specificity, respectively. Moreover, our device can separate *M. macrocopa* from *Branchinella thailandensis* population with 93-97% specificity. We also demonstrated isolation of *M. macrocopa* enriched with fluorescent bacteria from non-enriched *M. macrocopa* with 79-81% specificity.

## ACKNOWLEDGEMENTS

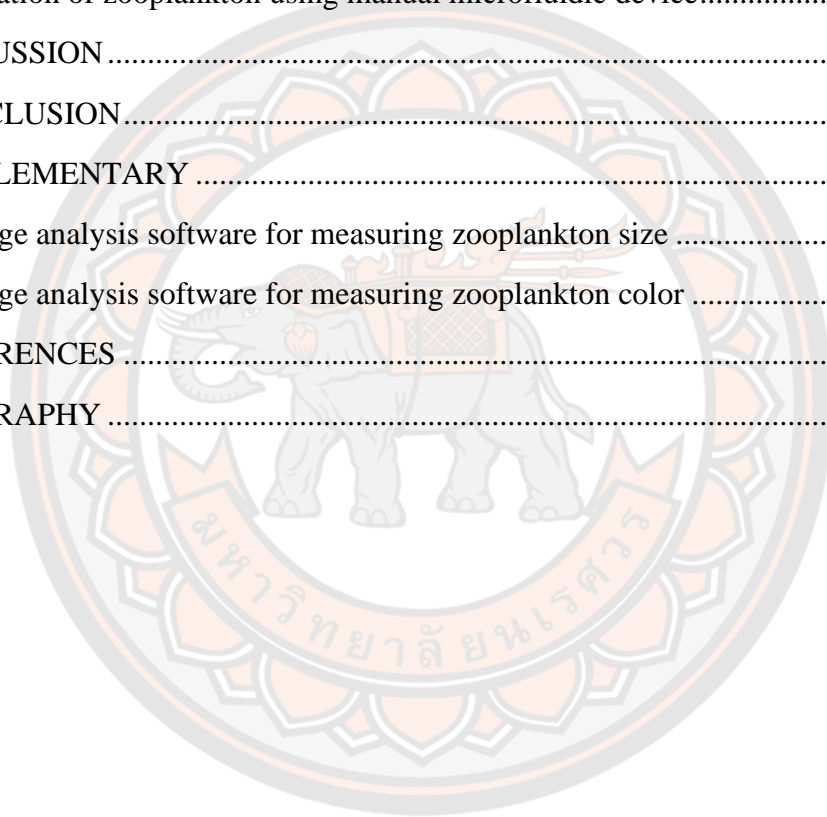
I would like to thank you to my advisor, Dr. Pakpoom Supsoontorn, Faculty of Medical Science, Naresuan University for your patience, guidance, and support. I have benefited greatly from your wealth of knowledge and meticulous editing. I am extremely grateful that you took me on as a student and continued to have faith in me over the years. I also could not have undertaken this journey without my committee members, Dr. Nukul Saengphan, Live feed Research Center, Suphanburi College of Agriculture and Technology, Asst.Prof.Dr. Amnat Phetrungnapha, and Asst.Prof.Dr. Chayaphon Sriphannam, Faculty of Medical Science, Naresuan University generously provided knowledge and expertise. Thank you to Asst.Prof.Dr.Thanathorn Phoka, Faculty of Science, Naresuan University for providing me his valuable suggestion regarding image analysis software. Thank you to Dr.Panwong Kuntanawat and Mr.Kriettisak Srisom, Suranaree University of Technology Institute of Agricultural Technology, for their valuable suggestions and necessary equipment for develop microfluidic device. Thank you to Dr.Sattaya Yimprasert for providing me his valuable suggestion regarding water control system. I am also grateful to my classmates for their support with full encouragement and enthusiasm. Lastly, I would be remiss in not mentioning my family, especially my parents. Their belief in me has kept my spirits and motivation high during this process. I would also like to thank my cat for all the entertainment and emotional support.

Dusitta Detkeow

# TABLE OF CONTENTS

	<b>Page</b>
ABSTRACT.....	C
ACKNOWLEDGEMENTS.....	D
TABLE OF CONTENTS.....	E
INTRODUCTION .....	1
Statement of problem.....	1
Objectives .....	2
Significance .....	2
Limitation .....	2
Definition of Terms .....	2
Hypothesis .....	2
LITERATURE REVIEW .....	3
Live feed .....	3
<i>Moina macrocopa</i> .....	4
<i>Branchinella thailandensis</i> .....	5
The diversity of zooplankton populations .....	7
Selective breeding.....	7
Heritability.....	7
Microfluidics.....	10
MATERIALS AND METHODS.....	16
Culture of zooplanktons.....	16
Preparing fluorescent-labeled bacteria .....	16
Design fabrication and operation of the microfluidic device .....	16
Water systems design .....	17
Measuring the distribution of zooplankton flow within the microfluidic device ....	17
Image analysis .....	17

Isolation of zooplankton .....	19
Data visualization and statistics .....	20
RESULTS .....	21
Microfluidic and water system design .....	21
Image analysis software .....	24
Isolation of zooplankton using microfluidic device and image processing software .....	24
Isolation of zooplankton using manual microfluidic device .....	26
DISCUSSION .....	28
CONCLUSION .....	32
SUPPLEMENTARY .....	33
Image analysis software for measuring zooplankton size .....	33
Image analysis software for measuring zooplankton color .....	37
REFERENCES .....	40
BIOGRAPHY .....	45



# INTRODUCTION

## Statement of problem

Zooplanktons are small aquatic animals at the foundation of aquatic food chains. Zooplanktons such as rotifer water flea, brine shrimp and fairy shrimp have been extensively used as live feeds in the aquaculture industry especially for aquatic larvae nurseries. Unlike instance feed, zooplanktons usually do not settle to the bottom and spoil the water. These zooplanktons are not only rich in protein and essential (Kibria et al., 1997) but also filled with enzymes and microbes that can stimulate feeding and digestion (Thongprajukaew et al., 2019). High quality live feeds provide essential nutrients (Kandathil Radhakrishnan et al., 2020) and boost the immunity of fish larvae, thereby increasing their growth and survival rates (Rawls et al., 2004; Sorgeloos et al., 2001). Additionally, certain pigments in live feed enhance the colors, thus improving the market value of ornamental fish (Sriputhorn & Sanoamuang, 2011).

Even within the same species, genetic variations in a population lead to phenotypic diversity. Zooplanktons from the same species and cultured in the same environment could have different size, morphology, biochemical and microbial composition (Macke et al., 2017; Sajesh Kumar et al., 2014). An ability to isolate and make measurements on individual zooplankton would allow us to study their diversity and improve their quality via selective breeding. However, studying and isolating individual zooplankton is difficult due to their small size and dense population.

Microfluidic technology enables efficient handling of a small fluid volume and particles. The technology has been used in many biological applications, ranging from biochemical analysis to separation and analysis of individual cells or microscopic organisms (Konry et al., 2010; Zhang et al., 2017). Previously, Ramanathan et al. used microfluidic devices for generating pH gradient to study swimming behavior and quantitatively determine zooplankton ecological preference. In these devices, the animals can freely move and choose their preferred zones (Ramanathan et al., 2015). Solis-Lemus et al. developed a microfluidic device and image processing pipelines for analyzing zooplankton swimming behaviors in response to the toxicity in the environment (Solis-Lemus et al., 2015). Schaap et al. developed a spiral microfluidic which was able to sort phytoplankton (Schaap et al., 2016). However, microfluidic technology has never been used for individual zooplankton isolation.

The objectives of this research are to develop a microfluidic tool for isolating zooplanktons that have desirable features and to develop a real-time image processing system for analyzing the characteristics of zooplanktons. Our system was adapted from microfluidic design by Srisom et al., previously used fungal spore isolation (Srisom et al., 2020). We reoptimized fluid control to be suitable for sorting swimming zooplanktons that are 0.5-2 mm in length. In this study, we used *Moina macrocopa* and *Branchinella thailandensis Sanoamuang* as models for zooplanktons in this study.

## Objectives

1. To develop a microfluidic tool for isolating zooplanktons that have desirable features
2. To develop a real-time image analysis system for characterizing the zooplanktons.

## Significance

Microfluidic devices could isolate the desired zooplankton for further study and to be selectively bred to obtain zooplankton with suitable characteristics for aquatic animals.

## Limitation

This study has potential limitations. Complex zooplankton characteristics, such as specific morphology or microbial composition, would require more sophisticated image analysis and microfluidic technologies to isolate them. We attempted to define the shape of *M. macrocopa* and *B. thailandensis* neonates using our automated image analysis, however it was unable to distinguish between their similar morphologies. For the gut microbe characterization, we attempted to use our automated image analysis, but it cannot distinguish between enriched *M. macrocopa* and normal *M. macrocopa* due to the low resolution of our portable microscope and the movement of zooplankton antennas.

## Definition of Terms

**Automated image analysis software** – The custom-made software that could measure the size and color of zooplankton in real time.

**Manual microfluidic** – The microfluidic device without the image analysis system.

## Hypothesis

Microfluidic devices and image analysis systems can be used to select zooplankton with desired characteristics and can be used as a platform to be applied in other species of small aquatic animals.

## LITERATURE REVIEW

### Live feed

Feed is a key factor in the aquaculture industry. It plays an important role in the promotion of growth and disease prevention. Feed provides nutrients, which provide energy for activity, growth, and all bodily activities such as swimming, digestion, and reproduction. There are several different types of aquaculture feeds, including artificial and natural feeds. The advantages of artificial feed were long shelf life, high nutrient content, easy to be consumed by aquatic animals, and easy to manage. However, some aquatic animal larvae do not consume artificial feed that sinks to the bottom or without movement. Live feed, natural feed have been used in the aquaculture industry, especially for aquatic larvae nurseries. Good quality live feed is a key element of the aquaculture industry. Suitable live feed for aquatic species helps reduce mortality (Sorgeloos et al., 2001), improve the color of the aquatic animal (Sriputhorn & Sanoamuang, 2011) and improve the immune system due to their communities of microorganisms (Rawls et al., 2004). Live feeds have a unique feature: they contain enzymes that stimulate the eating and digestion of aquatic animals (Thongprajukaew et al., 2019).

Live feed can be classified into two groups as follows:

1.1 Phytoplankton are autotrophic organisms that can produce their own food by consuming carbon from basic substances such as carbon dioxide and energy from light (photosynthesis) or inorganic chemical processes (chemosynthesis). Phytoplankton are both unicellular and multicellular. It is too small to be individually seen with the unaided eye. Examples of phytoplankton such as *Chlorella*, *Scenedesmus*, *Ankistrodesmus*, *Phacus*, *Ceratium*, *Pediastrum*, *Skeletonema*.

1.2 Zooplanktons, small aquatic animals that live in the water that are heterotrophic, meaning they cannot produce their own food. The zooplankton were both primary consumers, which eat floating phytoplankton, and secondary consumers, which feed on other zooplankton. Zooplanktons such as rotifers, water fleas, brine shrimp, and fairy shrimp have been extensively used as live feeds in the aquaculture industry especially for aquatic larvae nurseries. Due to newly hatched aquatic animal larvae still having an incomplete digestive system and lacking in enzymes. These zooplanktons are not only rich in protein and essential fat (Kibria et al., 1997) but also filled with enzymes and microbes that can stimulate feeding and digestion (Thongprajukaew et al., 2019).

Zooplankton must be in a compatible size with the mouth size of the aquatic larvae, or zooplankton cannot be swallowed. Since larvae are still weak to track the feed, the movement created by the zooplankton will be a great help, thus 'active' swimming zooplankton is preferred.

### The example of feeding aquatic animals with live feed.

The study of aquatic animal nutrition showed that live feeds had better growth and survival than artificial feeds. Mandal was studying the effect of partial or complete replacement of live feed (*Tubifex*) with artificial feed on Siamese fighting fish (*Betta splendens*). 300 *B. splendens* fry were equally separated into 5 different

groups. They were fed for 105 days with the following different diets: control 100% of live feed; 75% of live feed, 25% of artificial feed; 50% of live feed, 50% of artificial feed; 25% of live feed, 75% of artificial feed, and 100% of artificial feed. The average number of hatched larvae and fry survival after 2 weeks of rearing with 5 different diets were not significantly different. This research indicated that artificial feed may replace live feed *Tubifex* by 25% without affecting the growth, survival, and spawning performance of *B. splendens*, and by 50% without affecting the reproductive performance. However, artificial feed resulted in the lowest number of hatched larvae and fry production after two weeks of rearing. All this research demonstrated that the artificial feed could not successfully replace live feed 100%. It is a well-established fact that artificial feeds cannot compete with live feeds regarding acceptability, nutritional value, and other variables. Live feeds offer essential elements including proteins, carbs, fats, minerals, and vitamins that promote superior growth and survival compared to artificial feeds (Mandal et al., 2012).

Zooplankton has high nutritional value. It contains a valuable source of lipid and fatty acids, protein and amino acids, vitamins, and enzymes (Evjemo et al., 2003; Izquierdo et al., 2000; Pillay, 1990). These biochemicals from zooplankton lead to better growth, pigment enhancement, physiological regulation, immune stimulation, and better reproduction of brood-stock prawns and fishes (Altaff & Chandran, 1989; Manickam et al., 2017; Watanabe et al., 1983).

**Table 1 Nutritional value of zooplanktons (% dry weight)**

zooplankton	Protein	Fat
Rotifer	65.6	11.7
<i>Moina sp.</i>	68.1	9.1
<i>Artemia sp. larvae</i>	54.3	15.2
<i>Adult Artemia sp.</i>	58.8	9.0
<i>Branchinella thailandensis</i>	64.9	5.1
<i>Streptocephalus sirindhornae</i>	69.3	9.2

### ***Moina macrocopa***

*Moina macrocopa*, commonly referred as water fleas, are zooplankton, crustacean found in waters ranging from fresh to brackish, with temperatures ranging from 5 to 30 °C, and pH from neutral to slightly alkaline (Ivleva & Mercado, 1973). *Moina macrocopa* has been extensively used as live feed in the aquaculture industry, especially for aquatic larvae nurseries. Due to a high nutrient content, *Moina macrocopa* is a high-quality live feed and is compatible with the mouth size of the aquatic animal larvae. Adult *Moina macrocopa* has a size between 400–1,300 µm. The male is smaller than the female. A male *Moina macrocopa* has a size between 400–600 µm and a female has a size between 600–1,300 µm. Newly hatched *Moina macrocopa* has size less than 400 µm. *Moina macrocopa* is characterized by the head and carapace surface covered with long hairs, a broad, rounded head, without supraocular depression, post-abdomen with seven to ten lateral feathered teeth and one short bifid tooth nearly equal in length, anterior seta on the penultimate segment of the female's first trunk limb toothed, ephippium with two eggs and covered with polygonal cells. The male's first trunk limb has a large hook on the endopodite and a

long seta on the exopodite. *Moina macrocopa* can survive in low oxygen waters. Due to their ability to produce hemoglobin, they can live in oxygen-deficient environments. Hemoglobin production depends on the amount of oxygen dissolved in the water. In addition to a high population density and a high temperature, the synthesis of hemoglobin in *Moina macrocopa* may also be triggered by a high population density. *Moina macrocopa* feeds on various groups of phytoplankton, yeast, bacteria, and decaying organic matter. *Moina macrocopa* grows most rapidly in the phytoplankton feed.

*Moina macrocopa* reproduces both sexually and asexually. Generally, females reproduce asexually under optimal conditions. Under optimal conditions, *Moina macrocopa* breeds at just 2 days of age, with a brood size ranging from 4- 22 per female. Females produce between 2-6 broods every 1.5–2.0 days. Under adverse environmental conditions, *Moina macrocopa* reproduces sexually and males are produced, resulting resting egg formation (ephippia). The stimulation of the switching from asexual to sexual reproduction in populations of *Moina macrocopa* is lack of oxygen, food, and high density of *Moina macrocopa* population, resulting in an increase in resting egg production. The advantage of keeping the population well fed and in asexual reproduction is that the population density increases rapidly. The disadvantage of sexual reproduction is that fewer progenies are produced with resting eggs.



Figure 1. *Moina macrocopa*

### ***Branchinella thailandensis***

*Branchinella thailandensis* microcrustacean, more commonly known as the Thai fairy shrimp, is a planktonic species that belongs to the family Thamnocephalidae and the order Anostraca. Anostracans are easily identifiable by their elongated bodies, absence of a carapace, upside-down swimming motion in a metachronal pattern, paired compound eyes on stalks, and all similar appendages, which are used for both swimming and feeding. Males have unique spines on the gonopods, with a tip on a socket-like base. Accessory glands were not evident in histological sections. The ovaries of females are biramous, and their shell glands are

arranged in two paired, bilateral clusters. The glandular unit of each of these clusters is made up of two gland-cells and a single duct. *B. thailandensis* has been discovered in freshwater, Khon Kaen, Thailand. *Branchinella thailandensis* is filter feeding, feeding on various groups of phytoplankton, yeast, bacteria, and decaying organic matter.

*B. thailandensis* is oviparous and internal fertilization which produces shelled eggs (Plodsomboon et al., 2012). Their eggs, which were known as cysts, produced embryos that were resistant to their shells and dormant (Sukarawan & Boonsoong, 2013). These embryos are released from maternal females in a state of gastrula developmental arrest, or diapause. The resting eggs of *B. thailandensis* usually lie at the bottom of the water pond and hatch in suitable environmental conditions about 24 hours later. The life cycle of fairy shrimp is synchronized with a suitable environment for growth and reproduction (Chelvan & Munuswamy, 2011). The resting eggs of *B. thailandensis* won't hatch in unsuitable environments such as low oxygen, high population density, high/low temperature. Males and females reached maturity on day 7 after hatching and had total length between  $26.2 \pm 2.6$  and  $27.8 \pm 2.2$  mm in males and females, respectively (Dararat et al., 2011).

Recent studies showed that fairy shrimp could replace *Artemia sp.* as the most common live feed for aquaculture hatcheries due to their ability to live in freshwater. *B. thailandensis* has rapid growth, early maturity, large size, high fecundity, a short life span, and high nutritional composition (Dararat et al., 2011). *B. thailandensis* has high protein, essential amino acids, fatty acids, and carotenoid pigments (Chaoruangrit et al., 2017). *B. thailandensis* contains protein 64.65%, lipid 7.57%, carbohydrate 16.24%, fiber 5.12%, and ash 6.42%. *B. thailandensis* has a high carotenoid content of  $254.41 \mu\text{g/g}$ . The predominant amino acids found in *B. thailandensis* are lysine, phenylalanine, leucine, tyrosine, and glutamic acid. For fatty acids, linoleic acid C18:2n6, palmitic acid C16:0, linolenic acid C18:3n3, stearic acid C18:0, and oleic acid C18:1n9 are found to be major components. Carotenoid content examination reveals the presence of  $\beta$ -carotene, canthaxanthin, astaxanthin, and lutein. The presence of essential amino acids, fatty acids, and carotenoids showed that *B. thailandensis* is a high-quality live feed for aquaculture applications (Dararat et al., 2012).



Figure 2. *Branchinella thailandensis*

## **The diversity of zooplankton populations**

Genetic diversity is the different traits that are inherited within species. In a species with high genetic diversity, there would be many individuals with a wide range of characteristics. Genetic diversity is necessary for a population to adapt to the changing environment. Genetic diversity causes individuals to have different characteristics. The traits or characteristics of a parent can be passed to their offspring through their genes. As a result, organisms of the same species may be similar or different depending on the genes that they receive.

DNA is present in all creatures, and the DNA of each individual is organized into genes. This DNA contains the information to build the organism's bodies. Small differences in DNA might change the phenotype, such as eye color, hair color, and body pigment of fish. The genetic difference is caused by mutation and crossing-over in meiosis process. During the formation of egg and sperm cells (meiosis), crossing over is the process whereby DNA is exchanged between paired homologous chromosomes (one from each parent). This process produces new allele combinations in the gametes (egg or sperm), ensuring genetic variation in any offspring produced. Genetic diversity exists even in zooplankton that have sexual reproduction. Vikas studied *Artemia franciscana* nauplii length, which ranged from 400  $\mu\text{m}$  to 570  $\mu\text{m}$ . The observed phenotypic differences among the offspring were due to genetic differences between the parents because all *Artemia franciscana* was cultured under the same environmental conditions (Vikas, 2021).

## **Selective breeding**

Selective breeding is a process that humans use to develop new organisms with desirable characteristics. A breeder chooses two parents with beneficial phenotypic traits to produce offspring with desired traits. The examples of selective breeding in animals, for at least 14,000 years ago humans have been breeding the domestic dog (*Canis familiaris*). The domestic dogs, for example; were selectively bred from the wild gray wolf (*Canis lupus*) (Janssens et al., 2018). Humans were able to produce hundreds of different dog breeds by using selective breeding. Over time, as people domesticated and bred dogs, they favored specific traits, like small/large size or intelligence, for certain jobs, such as hunting, herding, or being a companion. As a result, many dog breeds have widely different appearances. Selective breeding in plant, agriculture has used selective breeding for thousands of years. Most fruits and vegetables that we have eaten are the result of artificial selection. *Brassica oleracea*, commonly known as wild cabbage, is the plant from which cabbage, broccoli, cauliflower, and Brussels sprouts are derived. Farmers were able to develop a variety of vegetables from a single source by isolating wild cabbage plants with specific characteristics. Each vegetable had a different flavor and texture. Broccoli, for example, is derived from wild cabbage with larger flower development, while kale is derived from wild cabbage with larger leaves.

## **Heritability**

The heritability of the trait has an important role in the genetic gain realized from selective breeding. The heritability of the trait determines the proportion of the selection differential that can be transferred on to progeny. In the narrow sense, it is

the ratio of genetic variance to phenotypic variance. High heritability in this context indicates a strong resemblance between parents and offspring regarding a specific trait, whereas low heritability indicates a low level of resemblance. Heritability has a value ranging from 0 to 1. High heritability which has a value greater than 0.4 (>40%). Moderate heritability, which has a value between 0.2-0.4 (20-40%). Low heritability, which has a value lower than 0.2 (20%).

Shirdhankar & Thomas were selective breeding for bidirectional selection for naupliar length in *Artemia franciscana*. The initial population was divided into two equal parts to be the small and large naupliar size groups. The criteria of selection were smaller naupliar size in the SNS line, larger naupliar size in the BNS line. After 15 generations of selection, the observed heritability values are of a moderate level. The pooled estimates of  $h^2$  from parent offspring regression in males and females were 0.2123 and 0.3885 in SNS and 0.5777 and 0.3364 in BNS. The corresponding values from full-sib data were 1.3256 and 1.1004 in SNS and 1.2580 and 1.4221 in BNS (Shirdhankar & Thomas, 2003).

Vikas also selectively bred in *Artemia franciscana* for nauplii size reduction. *Artemia franciscana* heritability estimates revealed generation to generation variation. Estimates of heritability were found to be very high. Heritability was  $0.99 \pm 0.36$  in the initial generation, while it varied between 0.36 and 1.64 in other generations. Nevertheless, the heritability estimates and standard errors associated with specific generations differed widely from the heritability of the entire population, and the standard error of the selected trait was  $0.96 \pm 0.01$ . The study of zooplankton heritability revealed that zooplankton had genetic diversity within species (Vikas, 2021).

### **Selective breeding in zooplankton**

Humans also selectively bred zooplankton to develop new organisms with desirable characteristics. The desirable characteristics of zooplankton, such as small size, high nutritional content, high growth rate, short life cycle, “hop-and-sink” swim or slow swimming, and resistance to infection. These desired characteristics depend on the requirements of cultured aquatic animals.

The example of selective breeding in zooplanktons. To develop zooplankton as a live feed to suitable feeding to fish larvae, Sajesh Kumar was selective breeding *Artemia franciscana* nauplii to reduce their size to compatible to fish larvae mouth. *Artemia franciscana* nauplii and the nauplii with small size were selected (approximately 10,000) by using a mesh filter of 500  $\mu\text{m}$ . The results show that the size of *Artemia franciscana* nauplii could be reduced from 517  $\mu\text{m}$  to 452  $\mu\text{m}$  (12.4%) during 13 generations of selective breeding. In addition, the polyunsaturated fatty acid (PUFA) content was increased from 18.04% to 37.25% during the selection (Sajesh Kumar et al., 2014).

Vikas also selectively bred in *Artemia franciscana* for nauplii size reduction. *Artemia franciscana* nauplii and the nauplii with small size were selected (approximately 15,000) by using different mesh filtering units of 500, 480, 450 and 400  $\mu\text{m}$ . The result shows that the size of *Artemia franciscana* nauplii could be reduced from 517  $\mu\text{m}$  to 439  $\mu\text{m}$  (14.9%) during 15 generations of selective breeding. In addition, cyst size was reduced from 225  $\mu\text{m}$  to 213  $\mu\text{m}$  (5%). Concurrently with

the reduction in nauplii and cyst size, significant increase in cyst hatching percentage (10%) was also realized as a correlated gain (from 54.4% to 64.58%) (Vikas, 2021).

Shirdhankar & Thomus et al., selectively bred *Artemia franciscana* for smaller and larger size. The initial population was divided into two equal parts to be the small and large naupliar size groups. The criteria of selection were smaller naupliar size in the SNS line, larger naupliar size in the BNS line. The mean naupliar lengths in the base population were 487  $\mu\text{m}$  in males and 491  $\mu\text{m}$  in females. After 6 generations of selection for smaller naupliar size in the SNS line, resulted in a phenotypic response of -45.32  $\mu\text{m}$  and -37.52  $\mu\text{m}$  decreases in naupliar size in males and females, respectively. In the BNS line, responses (increase in size) from five generations of selection for bigger size were 8.59  $\mu\text{m}$  and 35.80  $\mu\text{m}$ , respectively (Shirdhankar & Thomas, 2003).

The aquaculture potential of the tropical cyclopoid copepod *Apocyclops royi* was improved by Pan via the use of temperature acclimation and selective breeding. Both a high temperature of 28°C and a low temperature of 18°C were used to acclimatize two different copepod culture strains over a period of ten months, which corresponded to 40 and 15 generations, respectively. After acclimatization to the temperature, multigenerational observations of the effects of cold selection on copepods were carried out. The control and selection strains' female and nauplius lengths, nauplius production, and fatty acid concentrations were compared. The selective strain produced larger females, higher nauplii but smaller nauplii than the control strain. In the F1 generation, the selected strain had greater total fatty acid and omega 6 and omega 3 polyunsaturated fatty acid levels than the control strain. However, the fatty acid content gradually decreased in subsequent generations (Pan et al., 2017).

Souissi also selectively bred copepods, *Eurytemora affinis*. First, two different lines of copepods were long-term cultures at constant temperatures of 7°C (cold) and 20°C (warm). Then, both populations were transferred to a higher temperature of 24°C, which is suitable for aquaculture, and observed for 5 generations. Female body size and fertility declined dramatically throughout the first two generations (F1–F2) of a cold-acclimated population, whereas survival remained high. However, in F3, the survival rate decreased dramatically, allowing for the selection of robust individuals which fitness steadily increased in following generations. Compared to the warm acclimated population, the cold acclimated one showed higher fecundity, better lipid storage, and larger body size. After 5 generations at 24°C, the cold-acclimated population showed a significant genetic gain in prosome length compared to the warm acclimated population (Souissi et al., 2016).

All this research aims to improve zooplankton to suit aquatic animals. However, selective breeding in zooplanktons still lack information due to their small size, and a large population makes it difficult to study.

## Microfluidics

Microfluidics is a technology for manipulating and analyzing small volumes of fluid through a microchannel. Microfluidic have made their way into different fields such as physics, chemistry, engineering, and biotechnology. Previously, the applications of microfluidic technology have been focused on chemical analysis, for which it provides several distinct benefits, including reduced chemical consumption, decreased analysis time, reduced costs for use and disposal, portability, excellent control over reaction conditions, and improved analytical performance. Microfluidic chips are commonly fabricated by creating microchannels or chambers by enclosing thin grooves or small wells on the surface of one layer with a second layer. Channels need to be leak-proof, so the layers must be properly bonded. The channels are created via soft lithography, hot embossing, injection molding, micromachining, or etching, depending on the material chosen. PDMS has been used in many biological applications, as it is oxygen and water permeable. It is suitable for screening organisms.

Microfluidic technology has been applied previously to study both phytoplankton and zooplankton. Whether the study of toxicity, swimming behavior. Ramanathan studies swimming behavior and quantitatively determines zooplankton ecological preference. Ramanathan designed microfluidic devices which can generate different pH, salinity, and food on the device. In this device, the animals can freely move and choose their preferred zones (Ramanathan et al., 2015).

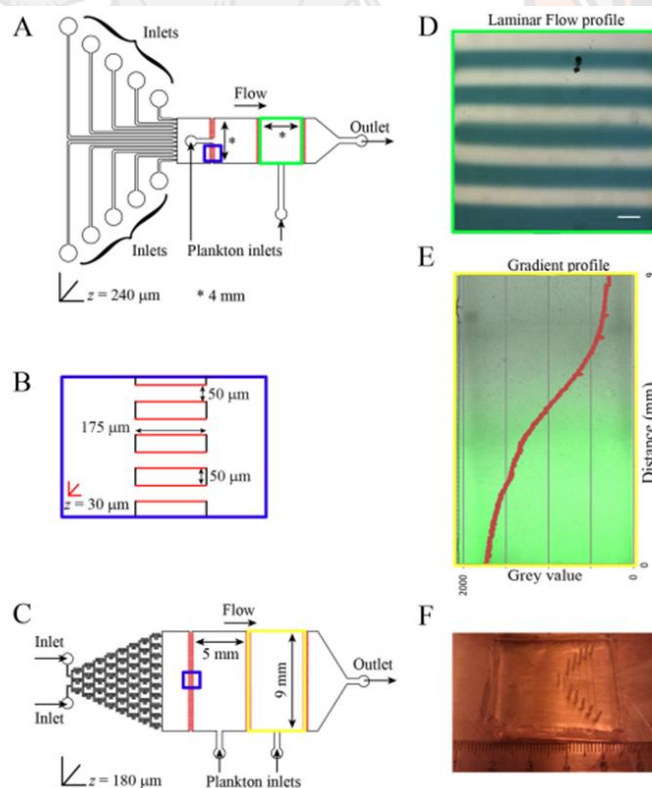


*Figure 3. Ramanathan's microfluidic device has been used to study swimming behavior and quantitatively determine zooplankton ecological preference.*

Ramanathan designed microfluidic devices which can generate different pH, salinity, and food on the device (Ramanathan et al., 2015).

Solis-Lemus developed a microfluidic device and an image processing pipeline for analyzing the movement of test specimens in image sequences. The system can use for assessing impact of the reference toxicant on swimming behavior of zooplankton (Solis-Lemus et al., 2015).

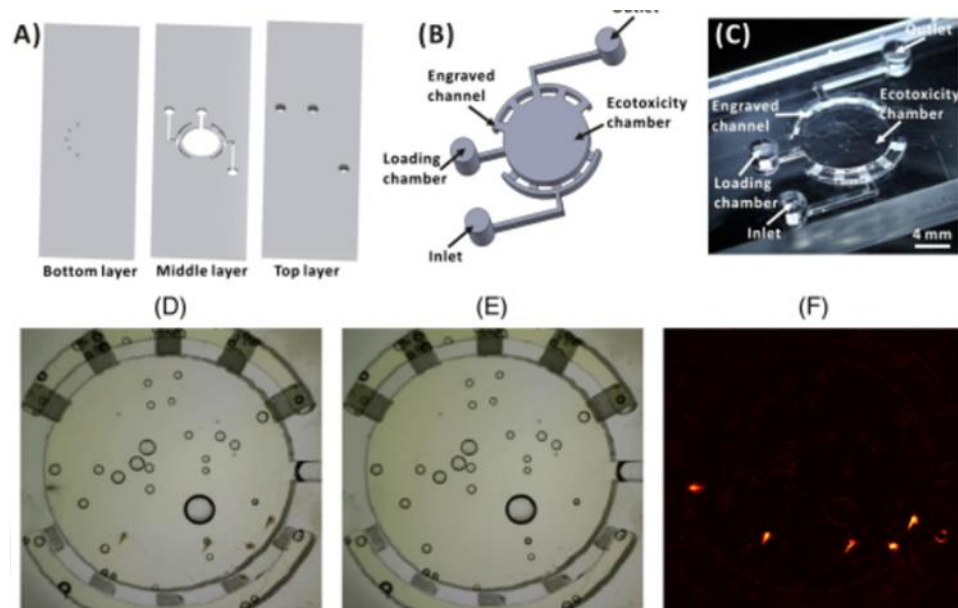


Figure 4. Solis-Lemus's microfluidic has been used to study impact of the reference toxicant on the swimming behavior of zooplanktons (Solis-Lemus et al., 2015).

Huang has developed a microfluidic chip that can rapidly test the toxicity of water based on the swimming changes of *Daphnia magna*. The first microfluidic consisted of 3 layers of PMMA that were optically aligned and then thermally bonded together. There were four fluidic modules on the 3D chip: (i) a rectangular chamber of  $8 \times 13 \times 1.5$  mm in width, height, and depth, respectively, (ii) an array of laser-ablated microchannels with a depth of approximately  $300 \mu\text{m}$ . Ablated array of microchannels effectively "caging" *Daphnia sp.* inside the test chamber, (iii) inlet and outlet channels connected to an array of microchannels and used for perfusion of media and toxicants, and (iv) auxiliary manifold for loading specimens directly into the "caging" chamber (Huang et al., 2015).

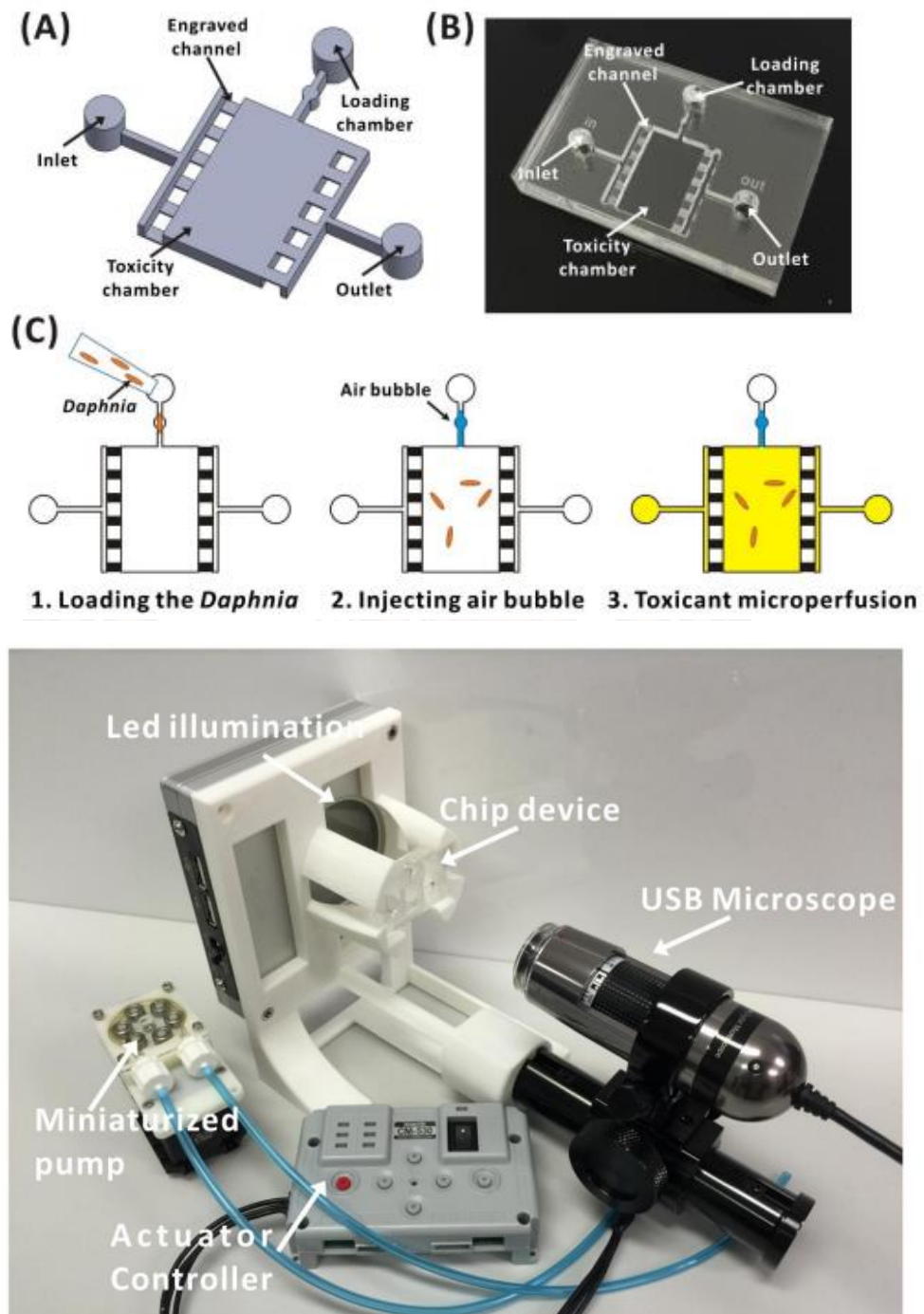


Figure 5. Huang's microfluidic chip for biotests performed on a freshwater crustacean, *Daphnia magna* (Huang et al., 2015).

The second microfluidic is composed of 24 cuboid test chambers ( $13 \times 8 \times 2$  mm in length, width, and depth, respectively) that are designed to keep multiple freely swimming specimens in a constant flow. The array's chambers were grouped into eight clusters of three, so that statistical duplicates of each test condition could be

used to get a full dose-response analysis. In a cluster of connected chambers, the inlet, outlet, and four groups of "caged" channels ( $1 \times 1.5 \times 0.3$  mm in width, length, and depth, respectively) were all shared. Animals were "caging" in the channels that were allowed to freely swim inside the chambers. To improve flow across a vertical plane of the chambers and increase the flow of fluid inside the chip device, the caging channels were made at different heights. Each chamber had its own way of loading specimens to be load in. The chip was 7 mm thick, had an inner volume of  $826 \mu\text{L}$ , and had an inner surface area of  $1362 \text{ mm}^2$ . Under continuous micro perfusion, Huang's microfluidic was able to maintain *Daphnia sp.* neonates in cages on a chip alive. Huang microfluidic is also cheap and simple to use (Huang et al., 2017).

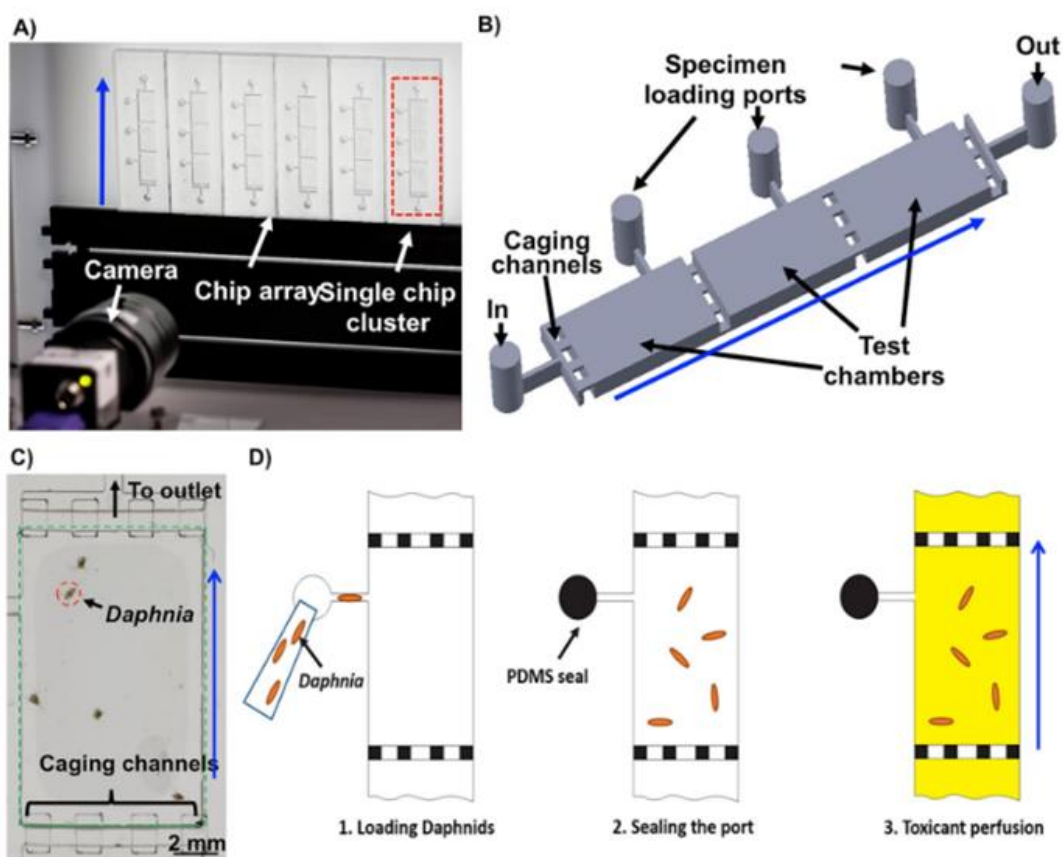


Figure 6. Huang's microfluidic chip for behavioral toxicity studies on *Daphnia magna* neonates (Huang et al., 2017).

However, all these microfluidics did not support selection. Recently, researchers developed a microfluidic for sorting phytoplankton.

Schaap developed a spiral microfluidic to sorting phytoplankton by shape and size in which lift forces and Dean flow drag forces combine to position the cells in a shape-dependent location in the channel cross section. Three species of phytoplankton were used for experiments: the high-aspect-ratio cylindrical *Monoraphidium griffithii*, the prolate spheroidal *Cyanothece aeruginosa*, and the small spherical *Chlorella vulgaris*. With this system, phytoplankton could be sorted with 77 % separation efficiency (Schaap et al., 2016).

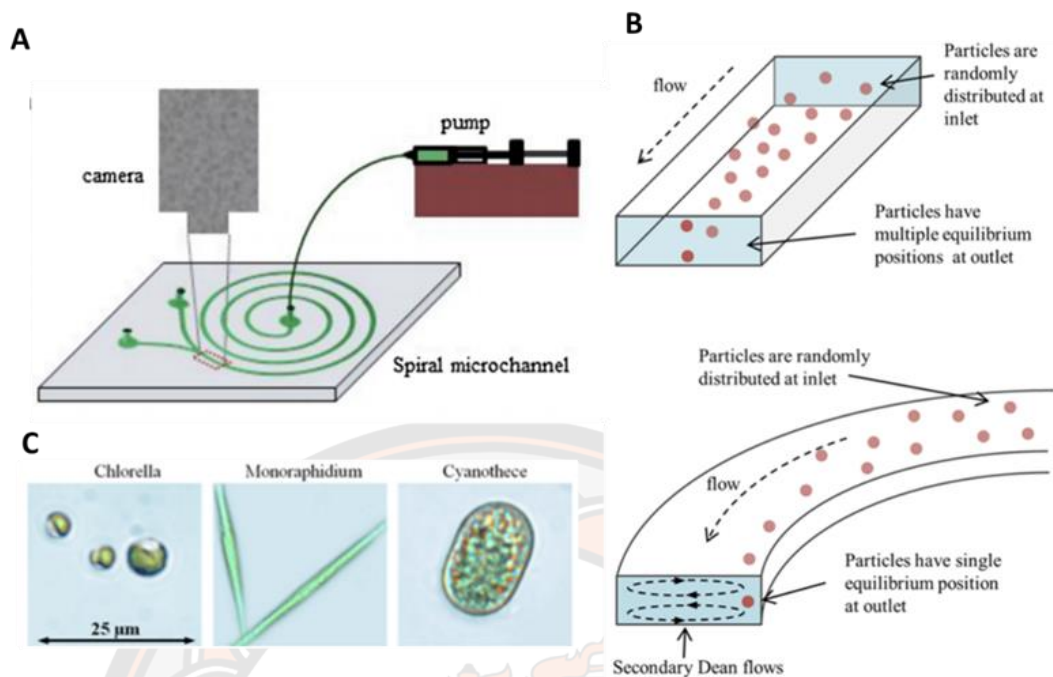
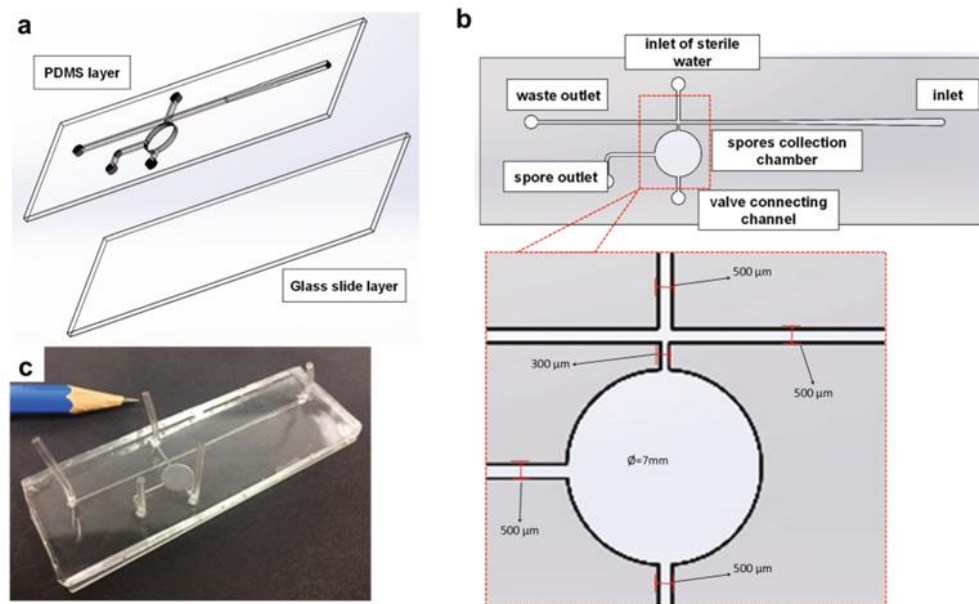


Figure 7. (A) Schaap's microfluidic device has been used to sort three species of phytoplankton: *Chlorella vulgaris*, *Monoraphidium griffithii*, and *Cyanotheca aeruginosa* (Schaap et al., 2016).

Srisom developed a microfluidic device for sorting fungal spores. The device consists of two layers of PDMS and a glass microscope slide. Different microchannel shapes support the functionality to manipulate particles within it and to separate the spores. The device is a single spore streamer equipped with a manual temporary flow diversion or MTFD mechanism to select single spores. Users can press a switch to generate MTFD when the spore arrives at the selection site. Then the targeted spore flows in a stream to the collection chamber. With this system, fungal spores could be sorted with 96.62% separation efficiency (Srisom et al., 2020).



*Figure 8. Srisom's microfluidic has been used to sort fungal spores. The device consists of 2 layers of a glass slide and the PDMS layer that embeds the channels. b the device microchannel. c the fabricated microfluidic chip (Srisom et al., 2020).*

## MATERIALS AND METHODS

### Culture of zooplanktons

The experiment was carried out at the Department of Biochemistry, Faculty of Medical Science, Naresuan University. Resting eggs of *Moina macrocopa* and *Branchinella thailandensis Sanoamuang* were purchased from Live Feed Research Center in Suphan Buri province. Both *M. macrocopa* and *B. thailandensis* in all experiments were hatched at 27-30°C in a Petri dish filled with 50 mL dechlorinated freshwater. For the shape isolation experiment, 100 *M. macrocopa* and 100 *B. thailandensis* neonates were collected and loaded into a zooplankton tank in a water siphon system. For size and color isolation experiments, *M. macrocopa* neonates were transferred to 10 L plastic containers with dechlorinated freshwater that was exchanged in 48 hours intervals at a density of 200 ind/L and fed approximately  $4 \times 10^6$  cells per mL of *Chlorella vulgaris* every 2 days at 27 - 30 °C and 12:12 (Light: Dark). After 7 days, 200 adult *M. macrocopa* were collected and loaded into the zooplankton tank in a water siphon system. For the microbial enrichment experiment, we prepared 200 adult *M. macrocopa* similar to that of size and color isolation experiments, but 100 individuals were enriched in fluorescent labeled bacteria.

### Preparing fluorescent-labeled bacteria

We use *Escherichia coli* SAR08/ptGFP previously engineered to express green fluorescent protein (GFP) (Wongpayak et al., 2021) to represent fluorescent-labeled microbes in zooplankton guts. Bacteria stocks were grown in Luria-Bertani broth (LB) medium at a 37°C 200 rpm shaker. After 18 hours incubation, bacterial cultures were spun down at 5000 rpm for 5 minutes. The supernatant was discarded, and the cell pellet was resuspended in fresh LB medium (OD 600 = 3). 100 adult *M. macrocopa* were enriched with 0.5 ml of *E. coli* SAR08/ptGFP suspension for 6 hr. 100 individuals of enriched and unenriched *M. macrocopa* were collected and loaded into a zooplankton tank in a water siphon system for the zooplankton's gut microbial isolation experiment.

### Design fabrication and operation of the microfluidic device

Our microfluidics was inspired by (Srisom et al., 2020). The microfluidic consisted of 5 layers: two layers of 5x 11 cm acrylic sheet cover two layers of PDMS that cover the acrylic channel layer. All layers are bound together with clear silicone. We designed the microfluidics using CorelDRAW™ graphic suite and cut acrylic sheets perforated 3 mm thick with an acrylic cutter (Laser cutting; BCL 1006 Grant) controlled by Auto laser V2.5.2. The device comprised: i) 2 mm inlet of zooplankton connecting to water siphon system, ii) 2 mm inlet of sterilized water connecting to water drop system, iii) a selection site under a portable microscope (Digital portable microscope (DM4 model, Magnification: 500/1000X Resolution: VGA; 1.3M; 2M; 3M, Video resolution: VGA; 720P, Light source: 8 LED lights, Focus range 10~40 mm.) connected to image analysis system, iv) a 14 mm zooplankton collection chamber, v) 1.5 mm valve with a channel connected to a solenoid valve controlled with an Arduino microcontroller, vi) 1.5 mm zooplankton outlet, and vii) an 2 mm

waste outlet. The PDMS sheet layer was made by mixing Elastomer Base and Curing Agent at 10:1 ratio. 6 volts vacuum pump was used to remove the air bubble. The PDMS sheets were solidified after incubating at 60°C for 2 hours.

### **Water systems design**

**Water siphon system.** The water siphon system consists of two bottles, a and b connected by a 1.3 cm- diameter pipe. Bottle a can contain 50 ml of water, with 6 volts pump constantly pumping water from the water reservoir into the water tank. The water level remained constant throughout the experiment. The water level of bottle a determines the water level of the zooplankton tank due to the connection of pipes, maintaining the same level of water in a and b bottle. 32  $\mu\text{m}$  filter between the water tank and the zooplankton tank prevented zooplanktons in the zooplankton tank from flowing into the water tank. The zooplankton tank and inlet of the microfluidic device were connected by a 5 mm diameter pipe.

**Water drop system.** The water drop system, developed from an IV set, consisted of a 410 mL water tank and a 6 volts pump that constantly pumps water from the water reservoir into the water tank till overflow, maintaining constant water level throughout the experiment. The water tank was 51 cm above the floor on a stage. The bottom of the water tank was connected to a 5 mm diameter, 26 cm long pipe, as well as a 3 mm diameter, 21.5 cm long pipe. A roller clamp can be adjusted to 6 levels. It is connected to a 5 mm, 19.3 cm long pipe. The end of the pipe is connected to the sterilized water inlet of the microfluidic device.

### **Measuring the distribution of zooplankton flow within the microfluidic device**

We started the water siphon system with a peristaltic pump connected to the waste outlet pipe. The peristaltic pump sucked the water from the zooplankton tank through the waste outlet pipe. When the water exited the waste outlet pipe, we removed the peristaltic pump and put the end of the waste outlet pipe into the beaker. We added the zooplankton in the zooplankton tank of the water siphon system at different densities. The stream from the water siphon system pushed the zooplankton from the zooplankton tank into the microfluidic device. The zooplankton flowed through the zooplankton inlet into a selection site. A portable stereomicroscope recorded 10-minute video of zooplankton flows at the selection site and sent it to a computer for image analysis.

### **Image analysis**

**Real-time automated estimation of zooplankton size and color.** We developed an image processing system based on OpenCV library. The zooplankton real-time video, recorded at the selection site of the microfluidic device, was first converted from RGB to Grayscale. We did background subtraction to track zooplankton location and create a zooplankton contour. The grayscale threshold was set to eliminate noise pixels.

To analyze the body sizes of zooplanktons, the number of pixels in the contour was counted. The edge around the contour was created to define the width and length

of the contour. The length was defined as the longest side of the edge. The width was defined as the shortest side of the edge. In real-time, the software highlights on a display screen which zooplanktons pass the selection criteria ( $<0.3$  or  $<0.4$  mm for width;  $<0.6$  or  $0.7$  mm for length).

To analyze the body color of zooplanktons, the threshold of gray filtered was set to not include zooplankton gut. The mean of grayscale within the zooplankton contour was counted. In real-time, the software highlights on a display screen which zooplanktons pass the selection criteria ( $<160$  or  $>160$  mean pixel value).

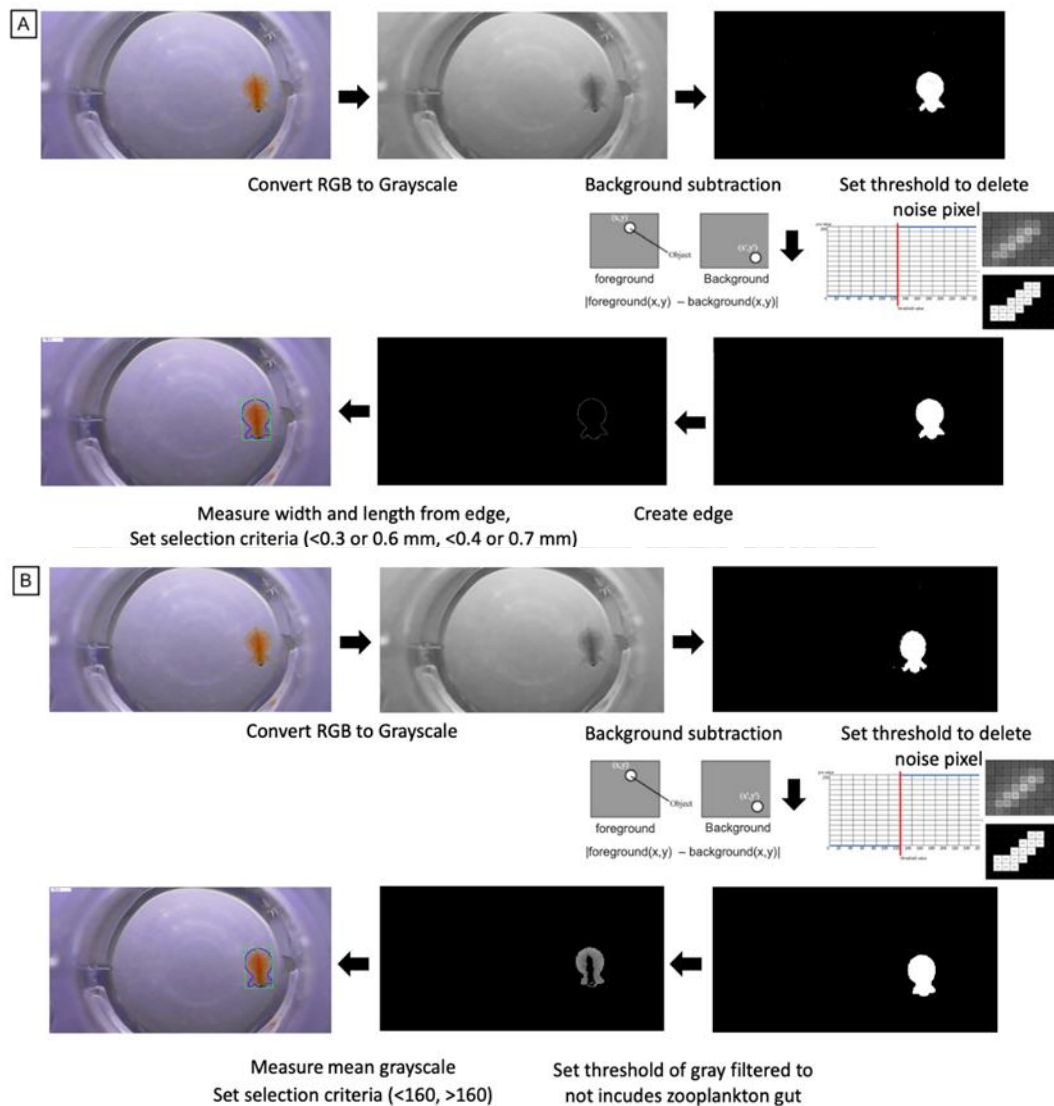


Figure 9. The image analysis process for measuring (A) size and (B) color of a zooplankton.

**Manual estimation of zooplankton size and color.** The image of a zooplankton was recorded and imported into ImageJ. For size measurement, we used imageJ 'straight' tool to find the distance between two points on the zooplankton

image. The length was defined as the length from the head to the base of the tail. The width was defined as the longest horizontal length in the horizontal. For color measurement, we first performed RGB thresholding to select the measurement area. In this process, the zooplankton gut wasn't included in the selection area. Next, the image was converted to grayscale. Then, the mean grayscale of the selection area was measured.

### **Isolation of zooplankton**

**Isolation by size and color using a microfluidic device and image analysis software.** The software estimated, in real-time, the length, width, and mean grayscale intensity of an individual zooplankton (*M. macrocopa*) passing through the selection site. If the estimated numbers of the zooplankton passed the selection criteria, the experimenter pulled the zooplankton into the collection chamber by activating the solenoid valve (via the microcontroller). If the estimated number did not pass the selection criteria, the experimenter let the zooplankton flow out into the waste outlet. To demonstrate our workflow, we tried the following selection criteria: i) width below 0.3 mm, ii) width below 0.4 mm, iii) length below 0.6 mm, iv) length below 0.7 mm, v) mean grayscale intensity below 160, vi) mean grayscale intensity above 160. For each selection trial, we attempted to select up to 20 individual zooplanktons that met the criteria.

**Isolation by shape using a manual microfluidic device.** To demonstrate our zooplankton shape isolation workflow, we mixed *M. macrocopa* and *B. thailandensis* neonates at 1:1 ratio. Then, we attempted to isolate 20 individuals of *M. macrocopa* or *B. thailandensis* neonates from the mix using our microfluidic device. The experimenter inspected an individual zooplankton passing through the selection site to identify its type (*M. macrocopa* vs *B. thailandensis*). The experimenter pulled the selected zooplankton into the collection chamber by activating the solenoid valve. Unselected zooplanktons simply flow out into the waste outlet.

**Isolation of zooplankton using a sieve.** To demonstrate zooplankton size isolation using a sieve, we randomly collected 20 individuals of *M. macrocopa* in the same batch culture. We filtered zooplankton by size with sieves (mesh size 0.3 mm) and then measured the size of an individual *M. macrocopa* that could pass the sieves by ImageJ.

To test how well sieving can separate *M. macrocopa* and *B. thailandensis* neonates, we first mixed *M. macrocopa* and *B. thailandensis* neonates at 1:1 ratio. We filtered zooplankton mixed with sieves (mesh size 0.2 or 0.3 mm) and then identified the type of an individual zooplankton that can or cannot pass the sieves. The experiment was repeated three times for each mesh size.

**Isolation by gut microbes using a manual microfluidic device.** To demonstrate the isolation of zooplanktons by their microbial contents, we mixed 100 non-enriched *M. macrocopa* and 100 *M. macrocopa* enriched with fluorescent labeled *E. coli*. We flowed the mixed population through our microfluidic device and illuminated the selection area with blue/ultraviolet light (395 nm). The experimenter inspected the fluorescent levels of individual *M. macrocopa* gut and attempted to isolate enriched from non-enriched population.

### **Data visualization and statistics**

Data visualization and statistical analysis were performed using R statistical computing software (<https://www.r-project.org/>). Scatter plots were generated using ggplot2 package. For mean comparisons, we performed a test for zooplankton isolation analysis using Welch Two Sample t-test in R.



## RESULTS

### Microfluidic and water system design

We developed a microfluidic and image analysis system for selecting and studying individual zooplanktons. We optimized the microfluidic design to allow for single flow of zooplanktons under continuous stream (Fig 10).

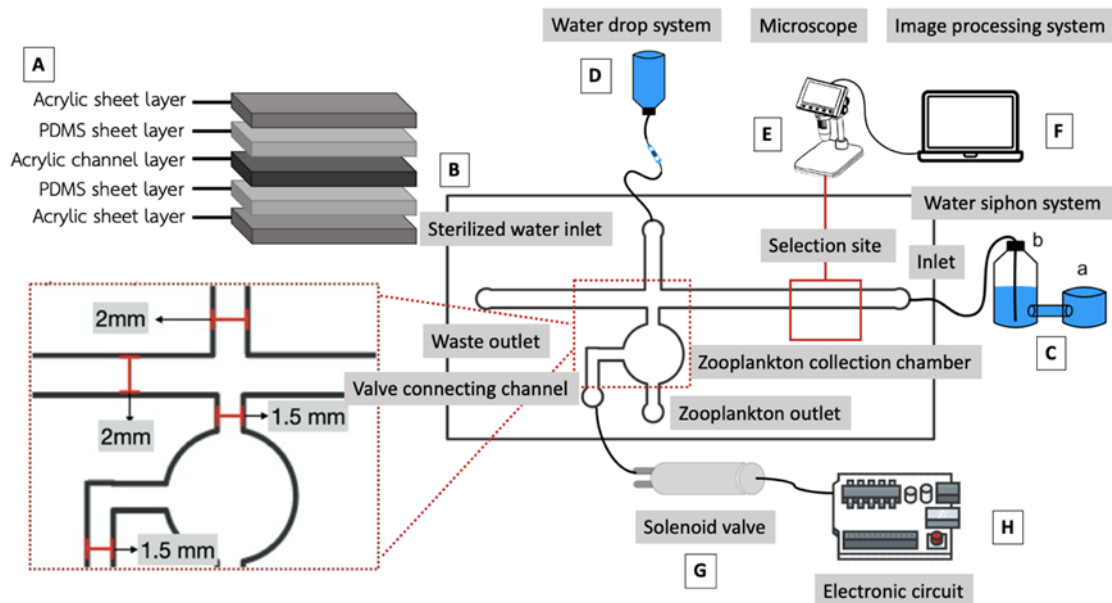


*Figure 10. We built a microfluidic device for isolating zooplankton. (A) The microfluidic chip consists of three acrylic and two PDMS layers glued together using transparent silicone and clamped with a bulldog clip. The acrylic channel layer in the middle has liquid flow channels while the two PDMS sheets serve as floor and ceiling of the flow channel. The external acrylic sheets protect PDMS sheets from dust as well as pressure from the bulldog clip. (B) The chip has two inlets from (C) a siphon system containing zooplanktons and from (D) a water drop system. (E) A portable microscope continuously images a selection site area of the chip and outputs data to (F) an image processing system. (G) A solenoid valve, connected to an Arduino controller, is used for pulling selected zooplanktons from the valve connecting channel to a zooplankton collection chamber.*

We designed a dual water system, the water siphon and the water drop system, to allow for optimization of plankton distribution in microfluidic devices. The water siphon system consists of a 50 ml water tank and a zooplankton tank. Both tanks are connected via a 1.3 diameter pipe. The height of water in the zooplankton tank is defined by the height of water in the water tank. The water drop system consists of a 410 ml water tank, a 0.3 diameter pipe, and a 6 levels adjustable roller clamp (Fig. 11). Water flow rate can be tuned, by adjusting the roller clamp, between 0-410 milliliter / minute. By changing the height of the water siphon system, we can also tune the flow rate from the siphon between 0-330 milliliter / minute (Fig. 12).

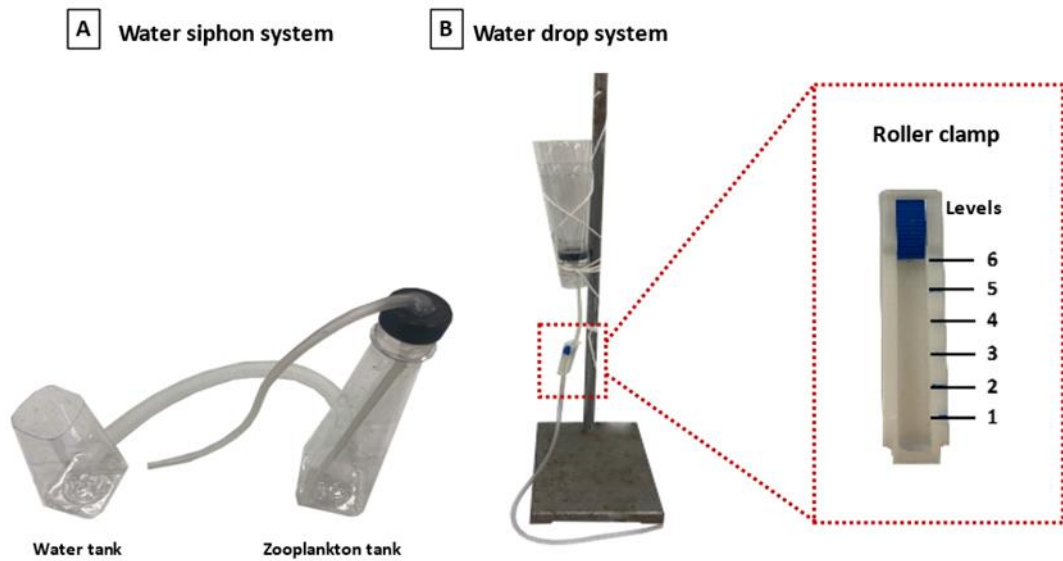


Figure 11. Water systems for flowing zooplankton. (A) The water siphon system consists of 50 ml water tank and zooplankton tank. Both tanks are connected via a 1.3 diameter pipe. (B) The water drop system consists of a 410 ml water tank, 0.3 diameter pipe, and 6 levels adjustable roller clamp.

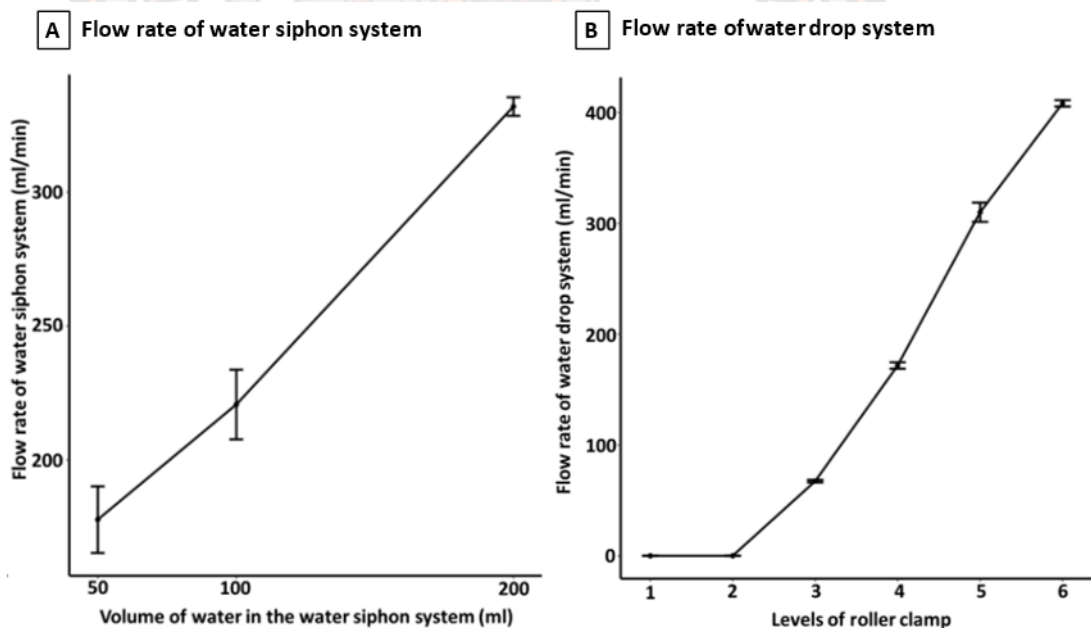


Figure 12. The flow control of the water system. The flow rate of the water siphon system is available to adjust at between 0-330 milliliter / minute by increasing the volume of water in the siphon system. The flow rate of the water drop system is available to adjust at between 0-410 milliliter / minute by tuning a roller clamp. The flow rate of the water drop system depends on the level of the roller clamp.

We decided to use water flow rates of  $67 \pm 1$  ml/min for the water drop system and  $178 \pm 12$  ml/min for the water siphon system. This optimal flow rate is fast enough

to prevent zooplanktons (*M. macrocopa* and *B. thailandensis*) from swimming up against the water current but slow enough for image analysis software and experimenters to analyze and select individual zooplanktons. Additionally, we need to adjust the distribution of zooplanktons in the flow streams by changing the density of zooplankton in the tank (Fig 13). The density of zooplankton suited for flowing zooplankton in the microfluidic chip was 2-10 ind/ml. Increasing zooplankton density shortens the interval between individual zooplankton arrival time to imaging and selection sites. Shorter interval times could allow for faster selection but may cause selection errors when multiple zooplanktons arrive simultaneously. The error rate of image processing was 10%, 16%, 14%, 9%, 11%, 31% at 2, 4, 6, 8, 10, 20 ind/ml. The error rate of image processing caused by the minimum frame difference is less than 10 frames. The error rate of each density was 4%, 4%, 14%, 6%, 8%, 22% at 2, 4, 6, 8, 10, and 20 ind/ml. The error rate of each density is caused by multiple zooplanktons arriving simultaneously.

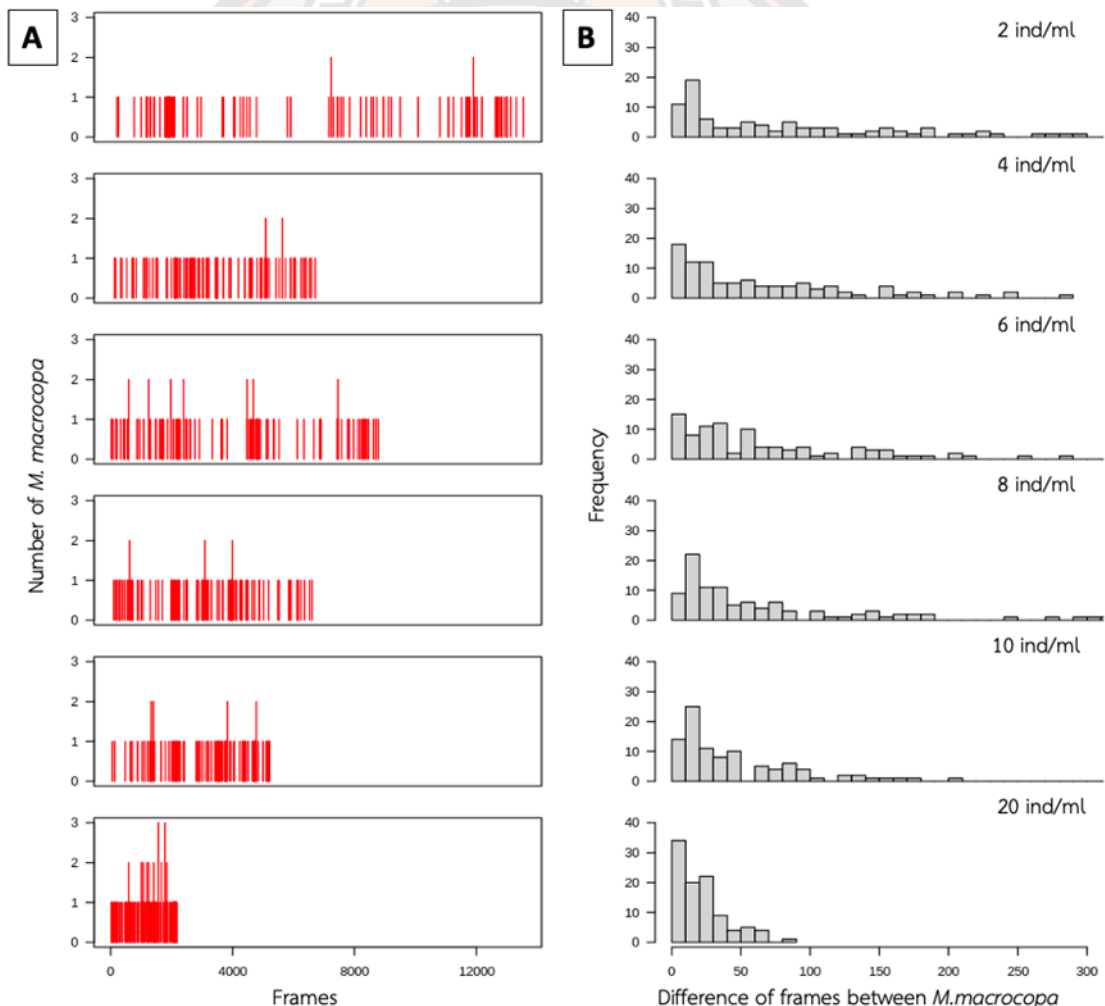


Figure 13. *M. macrocopa* flow distribution in the flow channel from the zooplankton tank with different *M. macrocopa* densities (2, 4, 6, 8, 10, and 20 individual/ml) (A) Numbers of *M. macrocopa* per image frame over time for the first 100 *M. macrocopa*

passing through the microfluidic imaging area. (B) Histogram of the distribution of frame difference between two individual *M. macrocopa* that flow consecutively in the flow channel. Note that the minimum frame difference that is needed to isolate *M. macrocopa* is 10 frames.

### Image analysis software

Next, we tested if our automated image analysis software could correctly estimate the relative size and color intensity of individual zooplanktons. We found that *M. macrocopa* lengths and widths automatically measured with our image processing software were well-correlated with those manually measured with ImageJ software ( $n = 40$ , Pearson's product-moment correlation,  $r^2 = 0.902$  and  $0.920$ , respectively). Mean grayscale color intensities measured with our image processing software were also well-correlated values measured manually with ImageJ software ( $n = 20$ , Pearson's product-moment correlation,  $r^2 = 0.840$ ) (Fig 14).

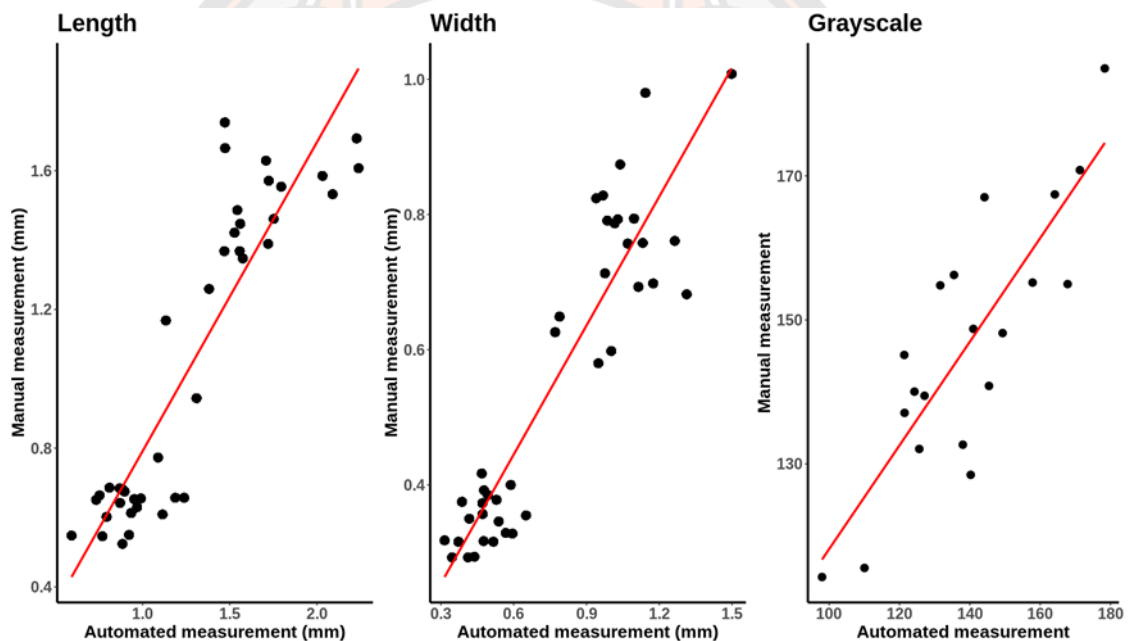


Figure 14. Plankton size and color measured with our automated software are well correlated with manual measurement. (A) lengths and (B) widths of small and large *M. macrocopa* were measured manually using imageJ and using our automated software. (C) mean grayscale pixel values of *M. macrocopa* were measured manually using imageJ and using our custom-made analysis software. Each dot represents measurement results from each individual *M. macrocopa*.

### Isolation of zooplankton using microfluidic device and image processing software

We used our microfluidic and image analysis system to assist zooplankton selection. To demonstrate zooplankton size selection, we attempted to isolate *M. macrocopa* with certain length ( $< 0.3$  mm or  $< 0.4$  mm) or width ( $< 0.6$  mm or  $< 0.7$  mm) criteria (Fig 15A-15B). The error rates for length and width selection were 20-25% and 15-25%, respectively. Welch's t-test indicated that mean lengths of the two

selected zooplankton groups ( $< 0.3$  mm and  $< 0.4$  mm selection) were significantly different ( $n=20$ , Welch's t-test, width p-value  $< 0.01$ , length p-value  $< 0.01$ ). So were the mean widths of the two selected plankton groups ( $< 0.6$  mm and  $< 0.7$  mm). We showed that regular sieve screening (using 0.3 mm sieve) cannot efficiently filter *M. macrocopa* with a size less than 0.3 mm, which *M. macrocopa* with a size greater than 0.3 mm could pass through the sieve. The error rates for width and length selection were 85-100%.

To demonstrate zooplankton color selection, we attempted to isolate *M. macrocopa* based on mean grayscale color intensity of individual *M. macrocopa* (Fig 15C). The error rate of color selection was 15-20%. The selection process resulted in two *M. macrocopa* populations whose mean grayscale intensities were significantly different ( $n = 20$ , Welch's t-test, p-value  $< 0.0001$ ).

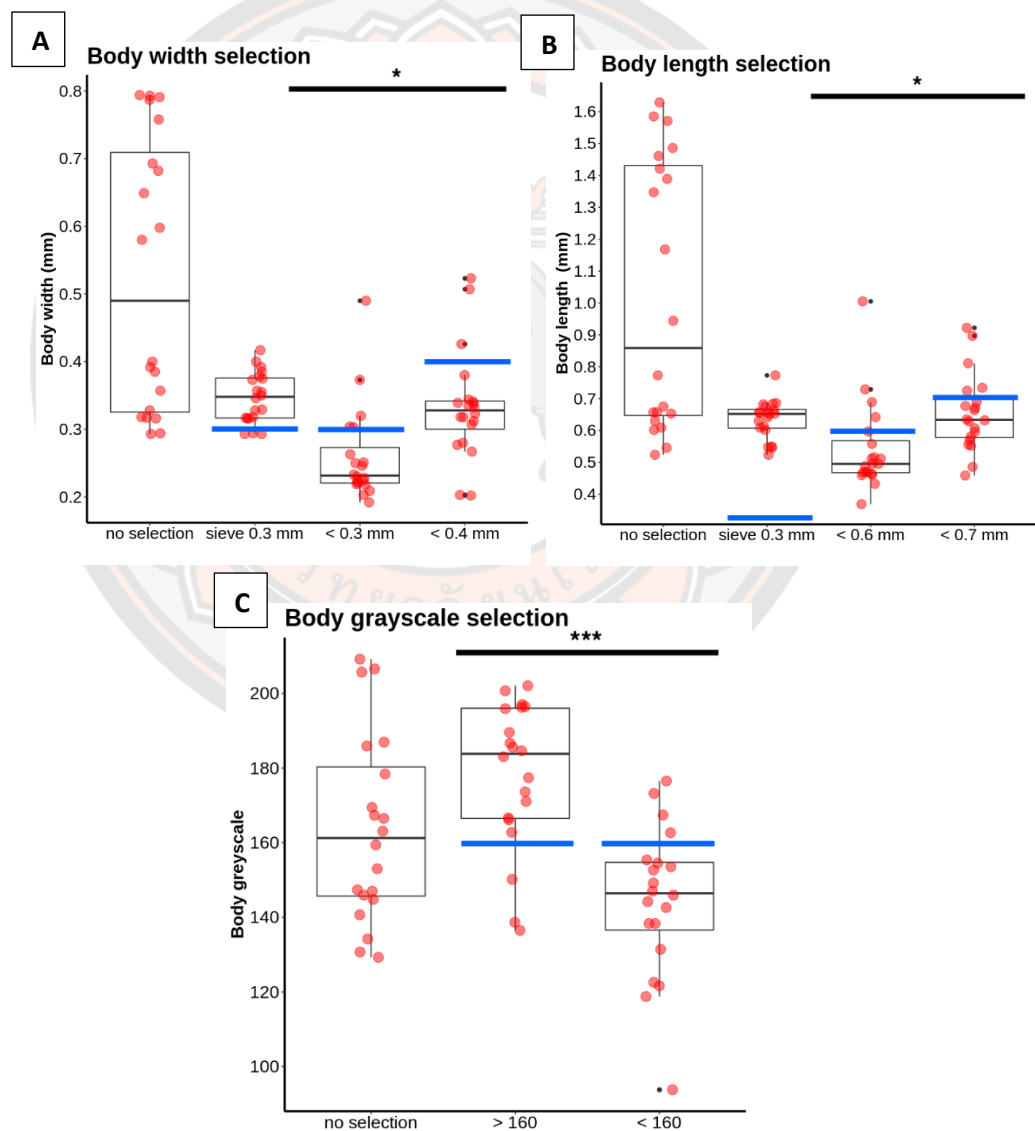


Figure 15. Our microfluidic and image analysis software can assist zooplankton isolation by width, length, and grayscale intensity. Isolation of zooplankton using microfluidic and image analysis software results in the changes in the distribution of

zooplankton body width (A), length (B) and body grayscale (C) In contrast, sieve-based size isolation of zooplankton is inefficient for isolating *M. macrocopa*. Each dot represents measurement results from each individual *M. macrocopa*. The error bars on box plots represent maximum and minimum data range. The middle lines are the median. The top and bottom of the rectangles are the third and first quartiles, respectively. The blue line shows the selection criteria cut-off. For (A) and (B), isolation specificity is defined as the fraction of dots below the blue line. For (C), isolation specificity for < 160 and > 160 group are defined as the fraction of dots above and below the blue lines, respectively. \* $p < 0.01$ ; \*\*\* $p < 0.0001$

### Isolation of zooplankton using manual microfluidic device

We then checked whether our system could assist separation of zooplanktons that have similar size but different morphology. As a test case, we attempted to use a mixed zooplankton population of *M. macrocopa* and *B. thailandensis* (Thai fairy shrimp) neonates. Both zooplanktons are 0.2 to 0.5 mm in size but *B. thailandensis* shape is more elongated. We showed that regular sieve screening (using 0.3 and 0.2 mm sieves) cannot efficiently separate the two populations (n=20, Welch's t-test, 0.3 mm sieve p-value = 0.823, 0.2 mm sieve p-value = 0.062) (Fig 16A-16B). On the contrary, our microfluidic systems could be used for assisting manual separation to these two zooplankton populations. We demonstrated that we could use our systems for separating these two zooplankton populations. Separation process resulted in two separated populations of zooplanktons that were significantly different (n=60, Welch's t-test, select *M. macrocopa* p-value < 0.0001, *B. thailandensis* p-value < 0.0001) (Fig 16C). Error rates for separating *M. macrocopa* from *B. thailandensis* or vice versa were 3-7%.

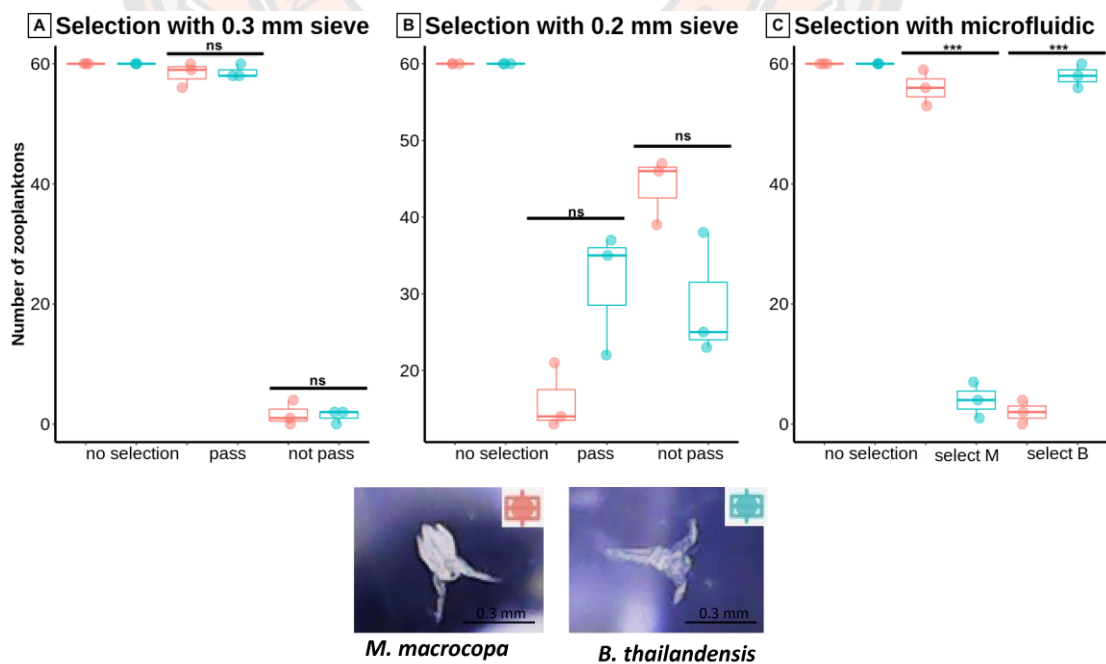


Figure 16. Microfluidics assist isolation of zooplankton by morphology. (A, B) Sieve screening cannot efficiently separate zooplanktons that have different morphologies but similar size (*M. macrocopa* and *B. thailandensis*). (C) Our microfluidic can assist

manual separation *M. macrocopa* and *B. thailandensis*. \*\*\*  $p < 0.0001$ ; ns = not significant

Lastly, we demonstrated the potential use of our system for studying zooplankton associated microbes. We showed that the system can assist the isolation of *M. macrocopa* enriched with fluorescently labeled *E. coli* from non-enriched *M. macrocopa* under UV light. The isolation process resulted in two isolated populations of zooplanktons that were significantly different ( $n = 60$ , Welch's t-test, select enriched *M. macrocopa*  $p$ -value  $< 0.0001$ , selected no enrich *M. macrocopa*  $p$ -value  $< 0.001$ ) (Fig 17). The error rate for isolation was 18-20%

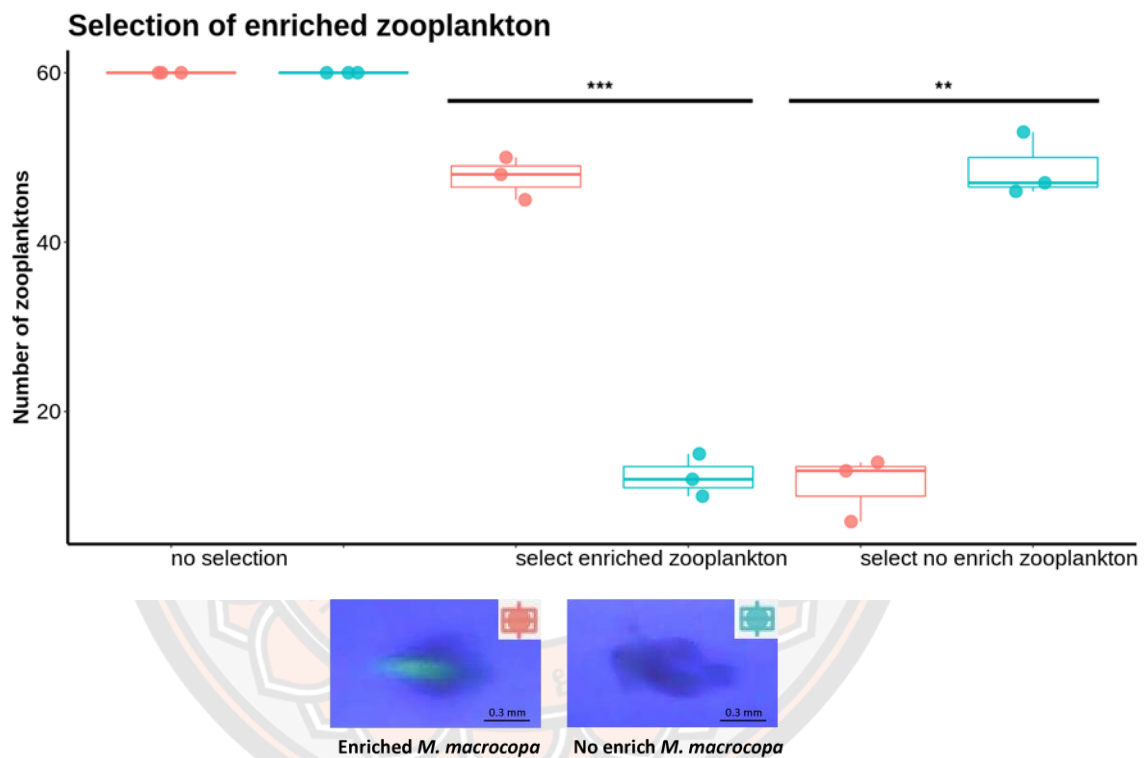


Figure 17. Microfluidics assist isolation of zooplankton by gut microbial. Our microfluidic can assist manual separation enriched *M. macrocopa* and non-enrich *M. macrocopa*. Images at the bottom of the plot show enriched and non-enrich *M. macrocopa* under blue/UV light. \*\* $p < 0.001$ ; \*\*\*  $p < 0.000$

## DISCUSSION

We successfully developed a microfluidic chip, a water control system, and the image analysis software for guiding the selection of zooplanktons. Unlike previous work, we used our microfluidic system for selecting, not culturing zooplanktons. Our automated image analysis pipeline was optimized to allow for size and color analysis. Size and color can be automatically measured, and the data can be used to guide the selection. Microfluidic systems have long been used for selecting small particles or cells, microfluidic selection of zooplanktons has at least two challenges, which we have overcome in this work. First zooplanktons such as *M. macrocopa* and *B. thailandensis* are relatively strong swimmers compared to single cell organisms such as green algae phytoplankton or bacteria or spores (which cannot really swim). We found that these zooplanktons sometimes attempt to swim against the water current. Zooplankton may abruptly shift directions in the flow channel and swim away from the collection chamber. Syringe pumps, commonly used for fluid control in microfluidic systems, could not provide strong enough water current to push zooplankton steadily forward ( $< 0.73 \mu\text{L} - 1500 \mu\text{L/hr}$ ). On the other hand, water current from a regular peristaltic pump and 6-volt water pump are too strong, pushing zooplankton too fast for image analysis. We applied simple water dropping and siphoning systems which allow for simple, low-cost, and wide range of water flow rate control for our zooplankton selection applications. With our water systems, there was no reverse flow zooplankton streamer. The flow rate of the water drop system can be tuned, by adjusting the roller clamp, between 0-410 milliliter / minute. By changing the height of the water siphon system, we can also tune the flow rate from the siphon between 0-330 milliliter / minute. We decided to use water flow rates of  $67 \pm 1 \text{ ml/min}$  for the water drop system and  $178 \pm 12 \text{ ml/min}$  for the water siphon system. This optimal flow rate is fast enough to prevent zooplanktons (*M. macrocopa* and *B. thailandensis*) from swimming up against the water current but slow enough to image processing software and experimenters to analyze and select individual zooplanktons. It could be complicated at the beginning to create the water stream from the water siphon system. To create the continuous water stream from the water siphon system, it needs a peristaltic pump to suck the water from the zooplankton tank through the waste outlet channel. Then disconnect the peristaltic pump from the waste channels when the water comes out. Additionally, we need water systems to adjust the distribution of zooplanktons in the flow streams by changing the density of zooplankton in the tank. Increasing zooplankton density shortens the interval between individual zooplankton arrival time to imaging and selection site. Shorter interval times could allow for faster selection but may cause selection errors when multiple zooplanktons arrive simultaneously. The error rate of image processing was 10%, 16%, 14%, 9%, 11%, and 31% at 2, 4, 6, 8, 10, and 20 ind/ml, respectively. The error rate of image processing caused by the minimum frame difference is less than 10 frames. The error rate of each density was 4%, 4%, 14%, 6%, 8%, and 22% at 2, 4, 6, 8, 10, and 20 ind/ml, respectively. The error rate of each density is caused by multiple zooplanktons arriving simultaneously. The density of zooplankton suited for flowing zooplankton in the microfluidic chip was 2-10 ind/ml.

Second, zooplanktons have relatively complicated morphology with multiple pairs of appendages, a segmented body, antennas, etc. Moreover, zooplankton movements alter the body's pose and the positions of body parts. Such complexity and

flexibility of morphology make it difficult to measure their size, shape, or color intensity. Our automated image analysis pipeline was optimized to allow for this type of analysis. Size, shape, and color can be automatically measured, and the data can be used to guide the selection. The combination of microfluidic technology with a computational framework offers several benefits. The algorithms allowed us to track each zooplankton's location, size, and color by analyzing changes of grayscale value in the frame. In addition, our automated image analysis system makes it possible to analyze the size and color of every zooplankton specimen as compared with other measurement methods where only random zooplankton in the large population are analyzed (Yuslan et al., 2021). Zooplankton length, width, and grayscale color intensity measured by our automated software were well correlated with the manual measurement values. For length and width measurement, the correlations between automated and manual measurements within small and large zooplankton groups were low. Nonetheless, we can clearly identify two distinct groups of zooplankton sizes from both automated and manual measurement. Conventionally, simple sieving can separate planktons by size. However, using sieves to isolate zooplankton according to size may be unspecific. Seda presented a probability of passing through a sieve. *Daphnia galeata* was isolated by using 0.42, 0.71, and 1.00 mm mesh. *Daphnia galeata* with a size of 0-1.114 mm can pass through a mesh of 0.42 mm, *Daphnia galeata* with a size of 0-1.717 mm can pass through a mesh of 0.71 mm, and *Daphnia galeata* with a size of 0-1.980 mm can pass through a mesh of 1.00 mm. The results showed that even *Daphnia galeata* that are larger than the mesh, can pass through it (Seda & Dostalkova, 1996).

Our microfluidic system can isolate *M. macrocopa* by size and color with 75-85% and 80-85% specificity, respectively. While these levels of specificity were on par or lower than those of several previously reported microfluidic sorters, we tackled different sets of sorting problems. Srisom et al. semi-automated microfluidic device sorts fungal spores with 97% specificity (Srisom et al., 2020). Nonetheless, these previous microfluidic systems only had to sort slow or non-swimming planktons or particles. We found that nearly all our selecting errors resulted from the unpredictable motion of individual zooplanktons at the imaging site or at the collecting chamber. Additionally, these previous works (Srisom et al., 2020) have not demonstrated an ability to sort plankton by color intensity, a property that could be relevant to further study of plankton chemical composition.

Isolating zooplanktons according to more complex phenotypes such as specific morphology or microbial composition would require more sophisticated image analysis and microfluidic devices. For the shape characterization, we tried to characterize it by using our automated image analysis, but it cannot characterize *M. macrocopa* and *B. thailandensis* neonates that have similar morphologies. For the gut microbe characterization, we tried to characterize it by using our automated image analysis, but it cannot characterize enriched *M. macrocopa* and normal *M. macrocopa* due to the limitations of our automated color analysis. Ortner et al. developed the use of silhouette photography methods to generate a permanent record of the contents of a plankton sample obtained using a net in the form of a contact print on photographic emulsion (Ortner et al., 1979). Plankton images could be studied, counted, and measured using a microscope or a computer-aided system that monitored a cursor's coordinates based on the timing of the arrival of a sound pulse created by the cursor

(Davis & Wiebe, 1985). Sieracki et al. developed an automated system for counting and measuring marine plankton, including flow cytometers and in situ plankton video recorders. It could analyze the microplankton cells, which range in size from 20 to 200  $\mu\text{m}$  (Sieracki et al., 1998). Duckworth et al. developed a method for automated, high-throughput measurements of size and growth in individual zooplanktons by using a spheroid counter. They could measure size automatically and provide calibration curves to translate size obtained on the spheroid counter to regular length measures. The linear relationships between spheroid counter diameter and organism length assessed manually under a microscope were all substantially different from zero ( $p < 0.0001$ ) (Duckworth et al., 2019). However, these methods were unable to analyze the morphological details of individual moving planktons. We demonstrated the isolation of zooplanktons (*M. macrocopa* and *B. thailandensis*) of similar size by their difference in morphologies. Still, we relied on experimenters' judgment for classifying planktons and manual control fluid diversion for isolating selected planktons. Future work should attempt to automate this process and possibly exploit techniques such as machine learning for real-time plankton identification.

Grosjean and Gorsky developed ZooScan hardware for making digital images of zooplankton samples and ZooProcess software for automatically measuring the size of zooplankton from the normalized image. Using Zooscan hardware together with ZooProcess and Plankton Identifier software, it could accurately measure the body size and classification of up to 1000 zooplanktons per image frame, which exceeds our image analysis software. However, the zooplankton sample must be incapable of movement since this method requires at least 150 seconds to analyze the plankton. Therefore, this method is not applicable for our work that analyzing flowing zooplankton since our automated software can analyze moving objects and requires at least 10 frames, or approximately 10 seconds, to assess zooplankton characteristics (Gorsky et al., 2010; Grosjean et al., 2004).

Intricate host-microbe relationships motivate several recent basic research and applications. Previous studies have demonstrated the critical roles of the zooplankton associated microbiome on the growth, survival, fecundity, and stress tolerance of their host (Macke et al., 2017; Peerakietkhajorn et al., 2016). Nonetheless, these studies only investigate zooplankton-microbe relationships at the population level. Microbiome studies in plants, large animals and human beings have already shown significant variations in microbiome across individual hosts, even for the same species living in the same environment (Blekhman et al., 2015; Fan et al., 2020; Wagner, 2021). Thus, individual zooplanktons within the same population are likely to have such microbiome variation. Our ability to isolate individual zooplanktons by their microbial variation would be essential for further exploring the zooplankton-microbe relationship. Here, we demonstrated the isolation of individual *M. macrocopa* by the amount of GFP expressing bacteria in their guts. Future studies may employ other techniques such as fluorescent in situ hybridization (FISH) for labeling of native microbes in zooplankton guts before microfluidic selections.

In this research, we successfully developed a microfluidic device for semi-automated isolation of zooplankton according to their characteristics. Our automated image analysis software was unable to characterize zooplankton by shape. As a result, the ratio is highly variable, even with the same zooplankton, due to the movement of the zooplankton antenna. Consequently, we cannot distinguish between *M.*

*macrocopa* and *B. thailandensis*. Due to the low resolution of the portable microscope, our automated image analysis software could not detect zooplankton fluorescent enriched while zooplankton was flowing in the microfluidic chip. However, the efficiency of the software can be further improved with machine learning, and it could potentially be developed into a fully automated system in the future. In addition, we developed a new design for a microfluidic system where equipment is contained inside a box. The entire box is portable and lightweight (3 kg). The equipment inside the box is simple to disassemble and reassemble. The water flow in closed system. This new design facilitates sensor attachment for the development of a fully automated system (Fig 18).

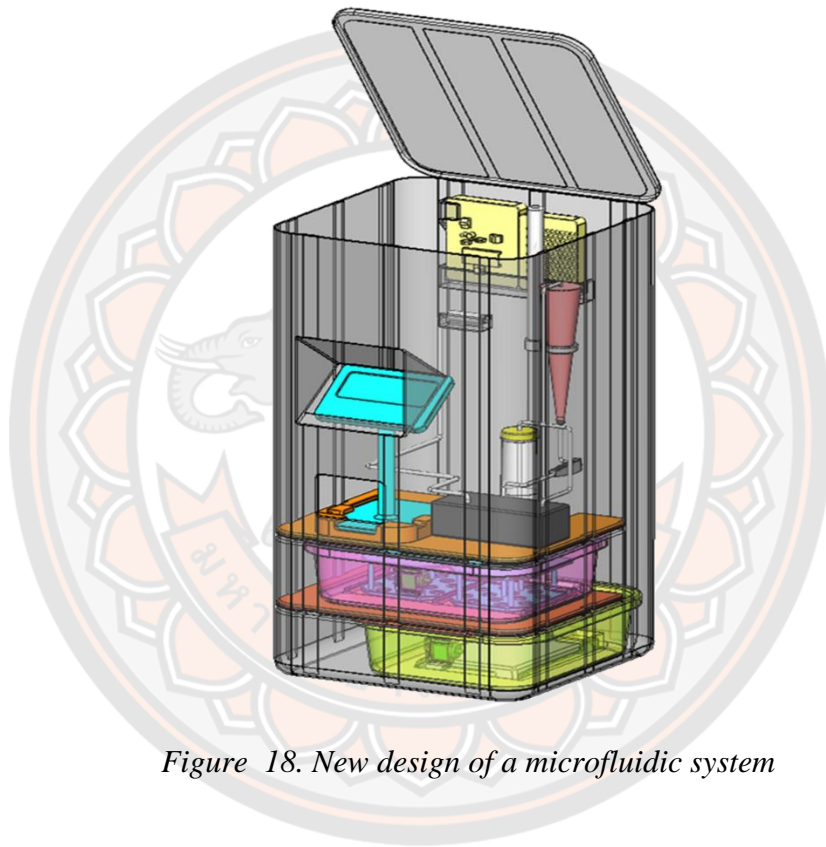


*Figure 18. New design of a microfluidic system*

## CONCLUSION

In this research, we successfully developed a microfluidic device and image analysis software for semi-automated isolation of zooplankton according to their characteristics such as size, color, shape, and microbial composition. The technology could facilitate the study and isolation of zooplanktons and offered more user-friendly operation than the conventional method. The efficiency of the method can be further improved, and it could be developed into a fully automated system



## SUPPLEMENTARY

### Image analysis software for measuring zooplankton size

```
import numpy as np
import cv2 as cv
import argparse
```

First, we import numpy and cv2 (OpenCV) packages.

Numpy is a Python programming language library. It provides a multidimensional array object with high performance and tools for managing these arrays.

OpenCV is a huge open-source library for computer vision. It provides machine learning and image processing in real time. It could be used to process images and videos in order to identify objects. When it is integrated with various libraries, such as NumPy, Python is capable of processing the OpenCV array structure for analysis. To identify an image pattern and its various features, we use vector space and perform mathematical operations on these features.

Argparse is one of the modules that can help in writing more professional and better-looking Python code.

### Capture the video from the computer's webcam

```
cap = cv.VideoCapture(0)
```

Next, we create **VideoCapture** objects from **cv.VideoCapture()**. This will return video from the computer's webcam.

### Create a parser and add arguments

```
parser = argparse.ArgumentParser(description='This program shows
how to use background subtraction methods provided by \OpenCV. You can
process both videos and images.')
parser.add_argument('--input', type=str, help='Path to a video or a
sequence of image.', default='cap')
parser.add_argument('--algo', type=str, help='Background subtraction
method (KNN, MOG2).', default='KNN')
args = parser.parse_args()
```

The **ArgumentParser** object will hold all the information necessary to parse the command line into Python data types. Filling an **ArgumentParser** with information about program arguments is done by making calls to the **add\_argument()** method. Generally, these calls tell the **ArgumentParser** how to take the strings on the command line and turn them into objects. This information is stored and used when **parse\_args()** is called.

### Create background subtractor objects

```

if args.algo == 'MOG2':
    backSub = cv.createBackgroundSubtractorMOG2()
else:
    backSub = cv.createBackgroundSubtractorKNN()

```

Background subtraction is a common technique for detecting moving objects in a series of images captured by stationary cameras. This method detects moving objects based on the difference between the current frame and the reference frame, also known as the 'Foreground Image' and 'Background Image'. To generate background subtraction, we use **if-else** statements to provide the background subtraction generating condition. Background subtraction was generated using the KNN or MOG2 algorithms.

### Create a trackbar

```

def on_change(self):
    pass

    cv.namedWindow('Params')
    cv.createTrackbar('Kernel', 'Params', 1, 21, on_change)
    cv.setTrackbarPos('Kernel', 'Params', 5)
    pause = False
    currWidth = 0
    currHeight = 0
    crop = 0

```

To create a trackbar, first we have to create the window **cv.namedWindow** in which it is going to be located. The OpenCV package provides **cv.createTrackbar()** function to read the current position of the trackbar slider. We can use **cv.getTrackbarPos()** function to change the position of trackbar using **cv.setTrackbarPos()**.

### Apply background subtraction to the captured video to detect the moving object

```

while(cap.isOpened()):
    rct, camera = cap.read()
    if rct == True:
        fgMask = backSub.apply(camera)
        rct, thresh1 = cv.threshold(fgMask, 120, 255, cv.THRESH_BINARY

```

To apply background subtraction, first we create **while** loops so that we can execute a set of statements as long as a condition is true. We apply background

subtraction on our captured video by using `backSub.apply()`. Then, the function `cv.threshold` is used to apply the thresholding. For every pixel, the same threshold value is applied. If the pixel value is smaller than the threshold, it is set to 0, otherwise it is set to a maximum value.

### Convolution (Image Filtering)

```
ksize = cv.getTrackbarPos('Kernel', 'Params')
kernel = np.ones((ksize, ksize), np.uint8)
```

A kernel is essentially a fixed size array of numerical coefficients along with an anchor point in that array, which is typically located at the center. `np.ones()` was used to create a new array of the specified shape and data type, with the element's value set to 1.

### Morphological transformations

```
closing = cv.morphologyEx(thresh1, cv.MORPH_CLOSE, kernel)
opening = cv.morphologyEx(closing, cv.MORPH_OPEN, kernel)
```

We used `cv.MORPH_CLOSE` to close small holes inside the foreground objects or small black points on the object. While `cv.MORPH_OPEN` is useful in removing noise.

### Find canny edges and contour

```
edged = cv.Canny(opening, 30, 200)
contours, hierarchy = cv.findContours(edged, cv.RETR_EXTERNAL,
cv.CHAIN_APPROX_NONE)
```

We used `cv.Canny` to detect the edges in an image and `cv.findContours` to find the contour.

### Find the biggest contour by the area(Altaff & Chandran, 1989)

```
im_with_keypoints = np.copy(camera)
if len(contours) != 0:
cv.drawContours(im_with_keypoints, contours, -1, 255, 3)
c = max(contours, key=cv.contourArea)
```

We use `np.copy` to get an array copy of a given object. To find the biggest contour, we use `max(contours, key=cv.contourArea)`.

### Define width and length on the contour

```

rotrect = cv.minAreaRect(c)
box = cv.boxPoints(rotrect)
box = np.int0(box)
(x, y), (width, height), angle = rotrect
w = min(width, height)
l = max(width, height)

```

To define width and length on the contour, we first use `cv.minAreaRect()` to find the minimum area rotated rectangle. Then we use `cv.boxPoints()` to create a box around the rectangle. Next we defined the shortest side as `w` and the longest side as `l`.

### Find the actual size of object

```

width = w * 6 / 772
length = l * 6 / 772

```

We calculate the actual size of an object from the reference object that we know the actual size. In this case, we use the well (96 well plate, diameter = 6 mm or 772 pixel) as a reference object.

### Set the selection criteria

```

if width < 0.3 and length < 0.6:
    cv.drawContours(frame, [box], 0, (0, 0, 255), 2)
    print(width, length)

```

To characterize the object, we set the selection criteria (<0.3 or <0.4 mm for width; <0.6 or 0.7 mm for length). The software will show the highlight on a display screen for the object that passes the selection criteria.

```

cv.rectangle(camera, (10, 2), (100, 20), (255, 255, 255), -1)
cv.putText(camera, str(cap.get(cv.CAP_PROP_POS_FRAMES)), (15, 15),
cv.FONT_HERSHEY_SIMPLEX, 0.5, (0, 0, 0))

```

The current frame number can be extracted from the video and stamped in the top left corner of the current frame using `cv.CAP_PROP_POS_FRAMES`. A white rectangle is used to highlight the black colored frame number.

### Showing the results

```

cv.imshow('Camera', camera)
cv.imshow('FG Mask', fgMask)
cv.imshow('Thres', opening)
cv.imshow('Canny Edges', edged)
cv.imshow('Keypoints', im_with_keypoints)

```

```

keyboard = cv.waitKey(30)
if keyboard == ord('q') or keyboard == 27:
    break
elif keyboard == ord('s'):
    pause = not pause
cap.release()
cv.destroyAllWindows()

```

To show the result, we use `cv.imshow()` to displays an image in the specified window. Then we use `cv.waitKey()` to display the image as the output on the screen until a keyboard event takes place.

#### Image analysis software for measuring zooplankton color

```

import cv2 as cv
import numpy as np
import argparse

```

```

cap = cv.VideoCapture(0)
parser = argparse.ArgumentParser(description='This program shows how to use
background subtraction methods provided by \OpenCV. You can process both
videos and images.')
parser.add_argument('--input', type=str, help='Path to a video or a sequence of
image.', default='cap')
parser.add_argument('--algo', type=str, help='Background subtraction method
(KNN, MOG2).', default='KNN')
args = parser.parse_args()

```

```

if args.algo == 'MOG2':
    backSub = cv.createBackgroundSubtractorMOG2()
else:
    backSub = cv.createBackgroundSubtractorKNN()

```

```

def on_change(self):
    pass
cv.namedWindow('Params')
cv.createTrackbar('Kernel', 'Params', 1, 21, on_change)
cv.setTrackbarPos('Kernel', 'Params', 8)
pause = False
currWidth = 0

```

```

currHeight = 0
crop = 0
cap = cv.VideoCapture(0)

while(cap.isOpened()):
    rct, camera = cap.read()
    if rct == True:
        fgMask = backSub.apply(camera)
        rct, thresh1 = cv.threshold(fgMask, 160, 255, cv.THRESH_BINARY)

        ksize = cv.getTrackbarPos('Kernel', 'Params')
        kernel = np.ones((ksize, ksize), np.uint8)
        closing = cv.morphologyEx(thresh1, cv.MORPH_CLOSE, kernel)
        opening = cv.morphologyEx(closing, cv.MORPH_OPEN, kernel)
        edged = cv.Canny(opening, 160, 200)
        contours, hierarchy = cv.findContours(edged, cv.RETR_EXTERNAL,
cv.CHAIN_APPROX_NONE)

        im_with_keypoints = np.copy(camera)
        gray = cv.cvtColor(camera, cv.COLOR_BGR2GRAY)
        gray_filtered = cv.inRange(gray, 80, 255)
        result = cv.bitwise_and(gray, gray_filtered, mask=opening)
        final = np.copy(result)

        if len(contours) != 0:
            cv.drawContours(im_with_keypoints, contours, -1, 255, 3)
            cv.drawContours(final, contours, -1, 255, 3)
            c = max(contours, key=cv.contourArea)
            rotrect = cv.minAreaRect(c)
            box = cv.boxPoints(rotrect)
            box = np.int0(box)

            mean = cv.mean(final, mask=opening)
            maxm = max(mean)
            print(maxm)

            if maxm < 160:
                cv.drawContours(camera, [box], 0, (-1, 255, 3), 2)

        cv.rectangle(camera, (10, 2), (100, 20), (255, 255, 255), -1)
        cv.putText(camera, str(cap.get(cv.CAP_PROP_POS_FRAMES)), (15, 15),
cv.FONT_HERSHEY_SIMPLEX, 0.5, (0, 0, 0))

    refinal = cv.resize(final, (680, 480))

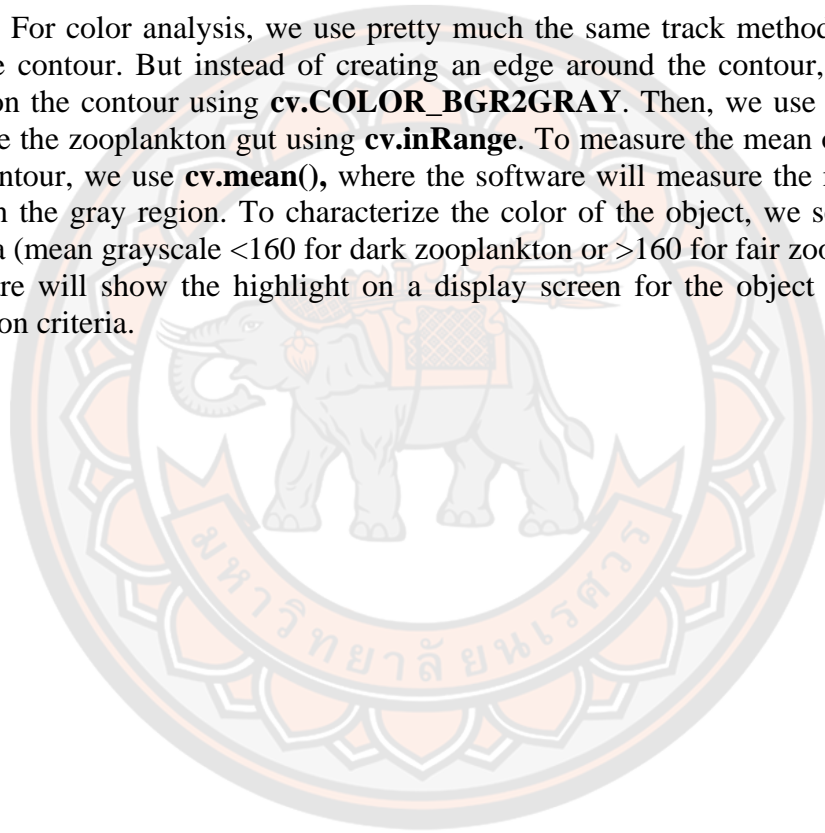
```

```
cv.imshow('Frame', camera)  
cv.imshow('final', refinal)
```

```
if cv.waitKey(1) & 0xFF==ord('q'):  
    break
```

```
cap.release()  
cv.destroyAllWindows()
```

For color analysis, we use pretty much the same track method till we finally get the contour. But instead of creating an edge around the contour, we put a gray filter on the contour using **cv.COLOR\_BGR2GRAY**. Then, we use thresholding to remove the zooplankton gut using **cv.inRange**. To measure the mean of gray-scale in our contour, we use **cv.mean()**, where the software will measure the mean grayscale only in the gray region. To characterize the color of the object, we set the selection criteria (mean grayscale <160 for dark zooplankton or >160 for fair zooplankton). The software will show the highlight on a display screen for the object that passes the selection criteria.



## REFERENCES

- Altaff, K., & Chandran, M. R. (1989). Sex-related biochemical investigation of the diaptomid, *Heliodiaptomus viduus* Gurney (Crustacea: Copepoda). *Proceedings: Animal Sciences*, 98(3), 175-179. <https://doi.org/10.1007/BF03179642>
- Blekhman, R., Goodrich, J. K., Huang, K., Sun, Q., Bukowski, R., Bell, J. T., Spector, T. D., Keinan, A., Ley, R. E., Gevers, D., & Clark, A. G. (2015). Host genetic variation impacts microbiome composition across human body sites. *Genome Biol*, 16, 191. <https://doi.org/10.1186/s13059-015-0759-1>
- Chaoruangrit, L., Tapaneeyaworawong, P., Powtongsook, S., & Sanoamuang, L.-o. (2017). Alternative microalgal diets for cultivation of the fairy shrimp *Branchinella thailandensis* (Branchiopoda: Anostraca). *Aquaculture International*, 26(1), 37-47. <https://doi.org/10.1007/s10499-017-0191-5>
- Chelvan, V., & Munuswamy, N. (2011). Morphological and molecular characterization of various *Artemia* strains from tropical salt pans in South East Coast of India. *Journal of American Science*, 7.
- Dararat, W., Lomthaisong, K., & Sanoamuang, L.-o. (2012). Biochemical Composition of Three Species of Fairy Shrimp (Branchiopoda: Anostraca) from Thailand. *Journal of Crustacean Biology*, 32(1), 81-87. <https://doi.org/10.1163/193724011x615352>
- Dararat, W., Starkweather, P. L., & Sanoamuang, L.-o. (2011). Life History of Three Fairy Shrimps (Branchiopoda: Anostraca) from Thailand. *Journal of Crustacean Biology*, 31(4), 623-629. <https://doi.org/10.1651/10-3410.1>
- Davis, C. S., & Wiebe, P. H. (1985). Macrozooplankton biomass in a warm-core Gulf Stream ring: Time series changes in size structure, taxonomic composition, and vertical distribution. *Journal of Geophysical Research*, 90(C5). <https://doi.org/10.1029/JC090iC05p08871>
- Duckworth, J., Jager, T., & Ashauer, R. (2019). Automated, high-throughput measurement of size and growth curves of small organisms in well plates. *Sci Rep*, 9(1), 10. <https://doi.org/10.1038/s41598-018-36877-0>
- Evjemo, J. O., Reitan, K. I., & Olsen, Y. (2003). Copepods as live food organisms in the larval rearing of halibut larvae (*Hippoglossus hippoglossus* L.) with special emphasis on the nutritional value. *Aquaculture*, 227(1-4), 191-210. [https://doi.org/10.1016/s0044-8486\(03\)00503-9](https://doi.org/10.1016/s0044-8486(03)00503-9)
- Fan, P., Bian, B., Teng, L., Nelson, C. D., Driver, J., Elzo, M. A., & Jeong, K. C. (2020). Host genetic effects upon the early gut microbiota in a bovine model with graduated spectrum of genetic variation. *ISME J*, 14(1), 302-317. <https://doi.org/10.1038/s41396-019-0529-2>
- Gorsky, G., Ohman, Cawood, A., Gasparini, S., Picheral, M., Prejger, F., Romagnan, J.-B., J. B., & Stemmann, L. (2010). Digital zooplankton image analysis using the ZooScan integrated system. *Journal of Plankton Research*, 32, 285–303. <https://doi.org/10.1093/plankt/fbp124>
- Grosjean, P., Picheral, M., Warembourg, C., & Gorsky, G. (2004). Enumeration, measurement, and identification of net zooplankton samples using the ZOOSCAN digital imaging system. *Ices Journal of Marine Science - ICES J MAR SCI*, 61, 518-525. <https://doi.org/10.1016/j.icesjms.2004.03.012>
- Huang, Y., Campana, O., & Wlodkowic, D. (2017). A Millifluidic System for Analysis

- of *Daphnia magna* Locomotory Responses to Water-born Toxicants. *Sci Rep*, 7(1), 17603. <https://doi.org/10.1038/s41598-017-17892-z>
- Huang, Y., Nugegoda, D., & Wlodkowic, D. (2015). Automation of daphtokit-F biotest using a microfluidic lab-on-a-chip technology. *Proceedings of SPIE - The International Society for Optical Engineering*. <https://doi.org/10.1117/12.2202396>
- Ivleva, I., & Mercado, A. (1973). Mass cultivation of invertebrates : biology and methods.
- Izquierdo, M. S., Socorro, J., Arantzamendi, L., & Hernández-Cruz, C. M. (2000). Recent advances in lipid nutrition in fish larvae. *Fish Physiology and Biochemistry*, 22(2), 97-107. <https://doi.org/10.1023/A:1007810506259>
- Janssens, L., Giemsch, L., Schmitz, R., Street, M., Van Dongen, S., & Crombé, P. (2018). A new look at an old dog: Bonn-Oberkassel reconsidered. *Journal of Archaeological Science*, 92, 126-138. <https://doi.org/10.1016/j.jas.2018.01.004>
- Kandathil Radhakrishnan, D., AkbarAli, I., Schmidt, B. V., John, E. M., Sivanpillai, S., & Thazhakot Vasunambesan, S. (2020). Improvement of nutritional quality of live feed for aquaculture: An overview. *Aquaculture Research*, 51(1), 1-17.
- Kibria, G., Nugegoda, D., Fairclough, R., Lam, P., & Bradley, A. (1997). Zooplankton: its biochemistry and significance in aquaculture. <http://hdl.handle.net/1834/25882>
- Konry, T., Dominguez-Villar, M., Baecher-Allan, C., Hafler, D., & Yarmush, M. (2010). Droplet-based microfluidic platforms for single T cell secretion analysis of IL-10 cytokine. *Biosensors & bioelectronics*, 26, 2707-2710. <https://doi.org/10.1016/j.bios.2010.09.006>
- Macke, E., Callens, M., De Meester, L., & Decaestecker, E. (2017). Host-genotype dependent gut microbiota drives zooplankton tolerance to toxic cyanobacteria. *Nat Commun*, 8(1), 1608. <https://doi.org/10.1038/s41467-017-01714-x>
- Mandal, S. C., Kohli, M. P., Das, P., Singh, S. K., Munilkumar, S., Sarma, K., & Baruah, K. (2012). Effect of substituting live feed with formulated feed on the reproductive performance and fry survival of Siamese fighting fish, *Betta splendens* (Regan, 1910). *Fish Physiol Biochem*, 38(2), 573-584. <https://doi.org/10.1007/s10695-011-9539-3>
- Manickam, N., Bhavan, P. S., & Santhanam, P. (2017). *Turkish Journal of Fisheries and Aquatic Sciences*, 17(3). [https://doi.org/10.4194/1303-2712-v17\\_3\\_07](https://doi.org/10.4194/1303-2712-v17_3_07)
- Ortner, P. B., Cummings, S. R., Aftring, R. P., & Edgerton, H. E. (1979). Silhouette photography of oceanic zooplankton. *Nature*, 277(5691), 50-51. <https://doi.org/10.1038/277050a0>
- Pan, Y.-J., Souissi, A., Sadovskaya, I., Hansen, B. W., Hwang, J.-S., & Souissi, S. (2017). Effects of cold selective breeding on the body length, fatty acid content, and productivity of the tropical copepod *Apocyclops royi* (Cyclopoida, Copepoda). *Journal of Plankton Research*, 39(6), 994-1003. <https://doi.org/10.1093/plankt/fbx041>
- Peerakietkhajorn, S., Kato, Y., Kasalicky, V., Matsuura, T., & Watanabe, H. (2016). Betaproteobacteria Limnohabitans strains increase fecundity in the crustacean *Daphnia magna*: symbiotic relationship between major bacterioplankton and zooplankton in freshwater ecosystem. *Environ Microbiol*, 18(8), 2366-2374. <https://doi.org/10.1111/1462-2920.12919>

- Pillay, T. V. R. (1990). *Aquaculture: principles and practices*. fishing news books.
- Plodsomboon, S., Sanoamuang, L.-o., Obregón-Barboza, H., & Maeda-Martínez, A. M. (2012). Reproductive cycle and genitalia of the fairy shrimp *Branchinella thailandensis* (Branchiopoda: Anostraca). *Journal of Crustacean Biology*, 32(5), 711-726. <https://doi.org/10.1163/193724012x638509>
- Ramanathan, N., Simakov, O., Merten, C. A., & Arendt, D. (2015). Quantifying Preferences and Responsiveness of Marine Zooplankton to Changing Environmental Conditions using Microfluidics. *PLoS One*, 10(10), e0140553. <https://doi.org/10.1371/journal.pone.0140553>
- Rawls, J. F., Samuel, B. S., & Gordon, J. I. (2004). Gnotobiotic zebrafish reveal evolutionarily conserved responses to the gut microbiota. *Proc Natl Acad Sci U S A*, 101(13), 4596-4601. <https://doi.org/10.1073/pnas.0400706101>
- Sajesh Kumar, N., Vikas, P., Thomas, P., Chakraborty, K., Jayasankar, J., & Vijayan, K. (2014). Quantitative genetic manipulation for nauplii size reduction of *Artemia franciscana* Kellogg, 1906 from Indian salinas and correlated changes in the polyunsaturated fatty acids (PUFA) profile. *Indian Journal of Fisheries*, 61(3), 69-73.
- Schaap, A., Dumon, J., & Toonder, J. d. (2016). Sorting algal cells by morphology in spiral microchannels using inertial microfluidics. *Microfluidics and Nanofluidics*, 20(9). <https://doi.org/10.1007/s10404-016-1787-1>
- Seda, J., & Dostalkova, I. (1996). Live sieving of freshwater zooplankton: a technique for monitoring community size structure. *Journal of Plankton Research*, 18(4), 513-520. <https://doi.org/10.1093/plankt/18.4.513>
- Shirdhankar, M., & Thomas, P. (2003). Response to bidirectional selection for naupliar length in *Artemia franciscana*. *Aquaculture Research*, 34, 535-541. <https://doi.org/10.1046/j.1365-2109.2003.00849.x>
- Sieracki, C. K., Sieracki, M., & Yentsch, C. S. (1998). An imaging-in-flow system for automated analysis of marine microplankton. *Marine Ecology-progress Series - MAR ECOL-PROGR SER*, 168, 285-296. <https://doi.org/10.3354/meps168285>
- Solis-Lemus, J., Huang, Y., Wlodkovic, D., & Reyes-Aldasoro, C. (2015). *Microfluidic environment and tracking analysis for the observation of Artemia Franciscana*. <https://doi.org/10.5244/C.110.###>
- Sorgeloos, P., Dhert, P., & Candreva, P. (2001). Use of the brine shrimp, *Artemia* spp., in marine fish larviculture. *Aquaculture*, 200(1), 147-159. [https://doi.org/https://doi.org/10.1016/S0044-8486\(01\)00698-6](https://doi.org/https://doi.org/10.1016/S0044-8486(01)00698-6)
- Souissi, A., Souissi, S., & Hansen, B. W. (2016). Physiological improvement in the copepod *Eurytemora affinis* through thermal and multi-generational selection. *Aquaculture Research*, 47(7), 2227-2242. <https://doi.org/10.1111/are.12675>
- Sriputhorn, K., & Sanoamuang, L. (2011). Fairy Shrimp (*Streptocephalus sirindhornae*) as Live Feed Improve Growth and Carotenoid Contents of Giant Freshwater Prawn *Macrobrachium rosenbergii*. *International Journal of Zoological Research*, 7(2), 138-146. <https://doi.org/10.3923/ijzr.2011.138.146>
- Srisom, K., Tittabutr, P., Teaumroong, N., Lapwong, Y., Phatthanakun, R., Sirivisoot, S., & Kuntanawat, P. (2020). New method for arbuscular mycorrhizal fungus spore separation using a microfluidic device based on manual temporary flow diversion. *Mycorrhiza*, 30(6), 789-796. <https://doi.org/10.1007/s00572-020-00986-4>

- Sukarawan, S., & Boonsoong, B. (2013). Internal structures of cryptobiotic cysts and embryonic development of Thai fairy shrimp *Branchinella thailandensis* Sanoamuang, Saengphan and Murugan, 2002. Proceedings of the 51st Kasetsart University Annual Conference, Bangkok, Thailand, 5-7 February 2013,
- Thongprajukaew, K., Pettawee, S., Muangthong, S., Saekhow, S., & Phromkunthong, W. (2019). Freeze-dried forms of mosquito larvae for feeding of Siamese fighting fish (*Betta splendens* Regan, 1910). *Aquaculture Research*, 50(1), 296-303. <https://doi.org/https://doi.org/10.1111/are.13897>
- Vikas, P. (2021). Reduction of Nauplii Size in an Allochthonous Artemia Strain through Selective Breeding. *J fisheriesci. com*, 15(04).
- Wagner, M. R. (2021). Prioritizing host phenotype to understand microbiome heritability in plants. *New Phytol*, 232(2), 502-509. <https://doi.org/10.1111/nph.17622>
- Watanabe, T., Kitajima, C., & Fujita, S. (1983). Nutritional values of live organisms used in Japan for mass propagation of fish: A review. *Aquaculture*, 34(1), 115-143. [https://doi.org/https://doi.org/10.1016/0044-8486\(83\)90296-X](https://doi.org/https://doi.org/10.1016/0044-8486(83)90296-X)
- Wongpayak, P., Meesungnoen, O., Saejang, S., & Subsoontorn, P. (2021). A highly effective and self-transmissible CRISPR antimicrobial for elimination of target plasmids without antibiotic selection. *PeerJ*, 9, e11996. <https://doi.org/10.7717/peerj.11996>
- Yuslan, A., Najuwana, S., Hagiwara, A., Ghaffar, M. A., Suhaimi, H., & Rasdi, N. W. (2021). Production Performance of *Moina macrocopa* (Straus 1820) (Crustacea, Cladocera) Cultured in Different Salinities: The Effect on Growth, Survival, Reproduction, and Fatty Acid Composition of the Neonates. *Diversity*, 13(3). <https://doi.org/10.3390/d13030105>
- Zhang, J., Yuan, D., Sluyter, R., Yan, S., Zhao, Q., Xia, H., Tan, S. h., Nguyen, N.-T., & Li, W. (2017). High-Throughput Separation of White Blood Cells From Whole Blood Using Inertial Microfluidics. *IEEE Transactions on Biomedical Circuits and Systems*, 11, 1422-1430. <https://doi.org/10.1109/TBCAS.2017.2735440>